AD-A152 020 SIMULATION OF A SYNCHRONOUSLY COUPLED ATMOSPHERE-OCEAN PREDICTION MODEL(U) NAVAL POSTGRADUATE SCHOOL MONTEREY CA P J ROVERO SEP 84 1/2

UNCLASSIFIED F/G 4/2 NL

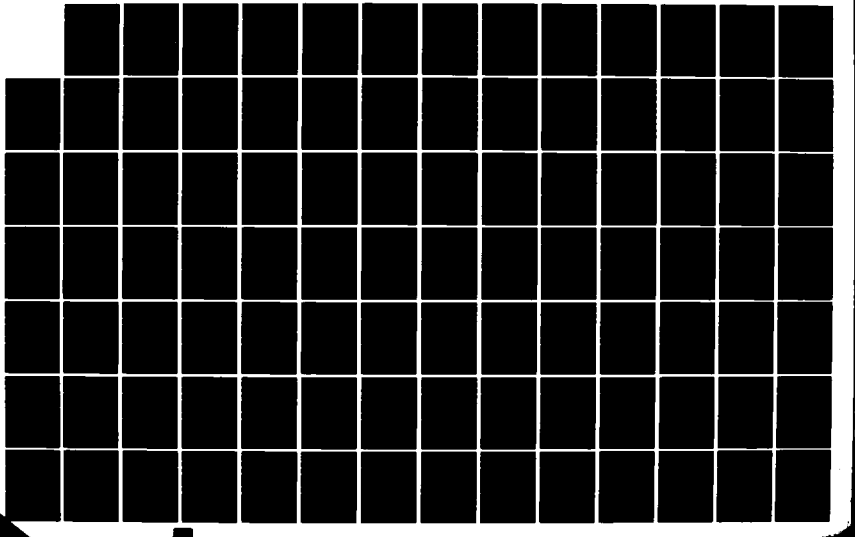

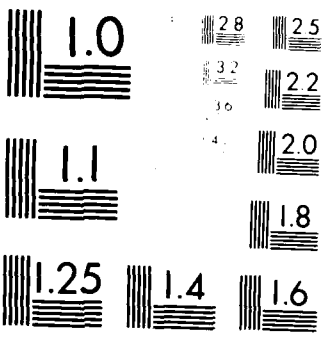

NAVAL POSTGRADUATE SCHOOL
Monterey, California

THESIS

IMPLEMENTATION OF A SYNCHRONOUSLY COUPLED
[illegible]-OCEAN PREDICTION MODEL

by

Peter Joshua Rovero

September 1984

Thesis Advisor: [illegible] Blakely

Approved for public release; distribution unlimited.

UNCLASSIFIED

SECURITY CLASSIFICATION OF THIS PAGE (When Data Entered)

REPORT DOCUMENTATION PAGE	READ INSTRUCTIONS BEFORE COMPLETING FORM
1 REPORT NUMBER	2 GOVT ACCESSION NO. AD-A152 020 / 3 RECIPIENT'S CATALOG NUMBER
4 TITLE and Subtitle: Simulation of a Synchronously Coupled Atmosphere-Ocean Prediction Model	5 TYPE OF REPORT & PERIOD COVERED: Master's Thesis; September, 1984
	6 PERFORMING ORG REPORT NUMBER
7 AUTHOR(s): Peter Joshua Rovero	8 CONTRACT OR GRANT NUMBER(s)
9 PERFORMING ORGANIZATION NAME AND ADDRESS: Naval Postgraduate School, Monterey, California 93943	10 PROGRAM ELEMENT, PROJECT, TASK AREA & WORK UNIT NUMBERS
11 CONTROLLING OFFICE NAME AND ADDRESS: Naval Postgraduate School, Monterey, California 93943	12 REPORT DATE: September 1984
	13 NUMBER OF PAGES: 97
14 MONITORING AGENCY NAME & ADDRESS (if different from Controlling Office)	15 SECURITY CLASS (of this report): Unclassified
	15a DECLASSIFICATION DOWNGRADING SCHEDULE

16 DISTRIBUTION STATEMENT (of this Report)

Approved for public release; distribution unlimited.

17 DISTRIBUTION STATEMENT (of the abstract entered in Block 20, if different from Report)

18 SUPPLEMENTARY NOTES

19 KEY WORDS (Continue on reverse side if necessary and identify by block number)

Atmosphere-Ocean Coupled Models
Sea-Surface Temperature

20 ABSTRACT (Continue on reverse side if necessary and identify by block number)

The purpose of this research is to explore the need for [illegible] sea-surface temperatures in atmospheric model [illegible] maps. Six and nine-layer versions of the Navy [illegible] Prediction System (NOGAPS) are used in this [illegible]. Several forecasts were made in which the sea-surface [illegible] is fixed in time. Test hindcasts were made [illegible] updated at each time step of the

DD FORM 1473 EDITION OF 1 NOV 65 IS OBSOLETE

UNCLASSIFIED

SECURITY CLASSIFICATION OF THIS PAGE When Data Entered

20 - ABSTRACT - (CONTINUED)

atmospheric model using interpolations of 12-hourly SST analyses. The 10-day predictions are compared to determine any improvement or degradation due to the time-dependent SST. Two cases are analyzed, one during November 1983 and another during April 1984. Use of the time-dependent SST's resulted in significant changes in the forecast fields of surface heat fluxes and precipitation which were physically consistent with the SST trend. Analysis of 15 storm forecasts revealed significant changes of storm track, duration or cyclogenesis in only 4 cases. Three of these cases were forecast by the nine-layer version of NOGAPS during the April period and one case was forecast by the six-layer NOGAPS during the November period.

Approved for public release; distribution unlimited.

Simulation of a Synchronously Coupled Atmosphere-Ocean Prediction Model

by

Peter Joshua Rovero
Lieutenant, United States Navy
B.S., University of Michigan, 1977

Submitted in partial fulfillment of the
requirements for the degree of

MASTER OF SCIENCE IN METEOROLOGY AND OCEANOGRAPHY

from the

NAVAL POSTGRADUATE SCHOOL
September 1984

Author: _____
Peter Joshua Rovero

Approved by: _____
Russell L. Elsberry, Thesis Advisor

_____
Chi-Sann Liou, Second Reader

_____
Robert J. Renard, Chairman,
Department of Meteorology

_____
John N. Dyer,
Dean of Science and Engineering

ABSTRACT

The purpose of this research is to explore the need for time-dependent sea-surface temperatures in atmospheric model predictions to 10 days. Six and nine-layer versions of the Navy Operational Global Prediction System (NOGAPS) are used in this study. Control forecasts were made in which the sea-surface temperature (SST) is fixed in time. Test hindcasts were made in which the SST was updated at each time step of the atmospheric model using interpolations of 12-hourly SST analyses. The 10-day predictions are compared to determine any improvement or degradation due to the time-dependent SST. Two cases are analyzed, one during November 1983 and another during April 1984. Use of the time-dependent SST's resulted in significant changes in the forecast fields of surface heat fluxes and precipitation which were physically consistent with the SST trend. Analysis of 15 storm forecasts revealed significant changes of storm track, duration or cyclogenesis in only 4 cases. Three of these cases were forecast by the nine-layer version of NOGAPS during the April period and one case was forecast by the six-layer NOGAPS during the November period.

TABLE OF CONTENTS

LIST OF FIGURES

ACKNOWLEDGEMENTS

I would like to express my gratitiude to Professors R. L. Elsberry and C. S. Liou for assistance and guidance during this research. Mr. P. Harr, Dr. T. Tsui and Dr. T. Rosmond provided expertise and assistance with running the SSIS and NOGAPS programs which was greatly appreciated. I would also like to thank LCDR P. J. Ranelli, who provided assistance in the early stages of this project, and the Fleet Numerical Oceanography Center and Naval Postgraduate School, which provided the considerable computer resources required in the course of this research.

I. INTRODUCTION

Atmosphere and ocean interaction is recognized as an important component of the atmospheric circulation on time scales of a month and longer. Air-sea interactions on shorter time scales, such as those over which numerical weather prediction (NWP) models are integrated, are less well understood. Operational atmospheric prediction models generally employ one-way ocean to air influence derived from a time-independent sea-surface temperature (SST) field. The quality of forecasts from such models declines rapidly when extended beyond five or six days. Many factors contribute to this observed degradation: inaccurate specification of the initial conditions; inadequate horizontal and vertical resolutions; inaccurate or simplistic parameterizations of atmospheric processes; and lack of two-way interaction between the atmosphere and ocean.

Sea-surface temperature changes alter the boundary forcing of atmospheric prediction models through the surface fluxes of sensible heat, latent heat and momentum. The heat fluxes are functions of the air-sea temperature difference and planetary boundary layer (PBL) conditions. These fluxes can also affect the radiation balance through parameterizations of cloud cover and water vapor content. The magnitude of the atmospheric response to changing SST's should be related to the magnitude and locations of SST changes. The nonlinear character of these relationships requires the use of a global atmospheric prediction model with sophisticated parameterizations of the interactions between surface fluxes, clouds, precipitation and radiative fluxes.

This work is the second in a series of case studies designed to study the necessity and feasibility of coupling

atmospheric and oceanic models. The first case study (Panelli, 1984) examined the response of 10-day atmospheric forecasts to observed SST changes introduced through simulated non-synchronous coupling. The temperatures at the sea surface were updated by replacing the initial SST's with the Fleet Numerical Oceanography Center (FNOC) SST analyses valid at 12-hour intervals during the forecast period. In this second step, simulated synchronous coupling is used to introduce observed SST's into the atmospheric model. Two cases, one each in the spring and autumn transition periods, are investigated. While a global model is used, the analysis is restricted to the northern hemisphere mid-latitude oceanic areas and the effects of changing SST's on the atmospheric model 10-day predictions.

II. BACKGROUND

Current operational NWP models fall far short of the approximately 15-day theoretical limit of atmospheric predictability (Rosmond et al. 1983). Many methods are being proposed and tested to incrementally improve existing models. These include improved numerical differencing schemes, spectral model formulation, increased vertical and horizontal resolution, improved initialization techniques, and more accurate parameterization of diabatic processes. While efforts in these and other areas will ultimately be required in the process of NWP model improvement, the present study will concentrate on the effects of diabatic processes in NWP models.

Diabatic processes become more important in determining atmospheric circulations at long time scales. At shorter time scales (1-3 days), dynamic processes seem adequate as the primary forcing in NWP models. Diabatic processes begin to become important in medium time scales (5-15 days), and tend to dominate the long time scale (15-30 days and beyond) forecast problem. Because the ocean is a major heat and moisture source, the air-sea fluxes are very important in modeling diabatic processes.

Latent and sensible heat fluxes across the sea surface are modelled as functions of air-sea temperature differences. While Sandgathe (1981) concluded that maritime cyclogenesis required accurate specification of air-sea fluxes, no operational model includes time-dependent SST. The European Center for Medium-range Weather Forecasts (ECMWF) and the United States National Meteorological Center (NMC) use the NMC weekly global SST analysis in initialization. The FNOC NOGAPS model is initialized by 12-hourly SST

analyses produced by the Thermodynamic Ocean Prediction and Expanded Ocean Thermal Structure Systems (TOPS-EOTS) described by Clancy and Pollack (1983). Without a time-dependent specification of SST, the model representation of air-sea interface fluxes and cyclogenesis is bound to deteriorate with increasing forecast time.

Significant SST changes can occur during 5-15 day periods. Atmospheric forcing causes large SST changes during the spring and autumn transition periods (Camp and Elsberry, 1978; Elsberry and Camp, 1978; Elsberry and Raney, 1978). During these periods, warm shallow oceanic mixed layers are mechanically mixed, deepen and cool. Winter SST changes are generally smaller than transition changes because of a deeper ocean mixed layer. Summer SST changes are smaller due to decreased mechanical mixing (fewer and less intense storms). The intensity and orientation of SST gradients associated with western boundary currents are important in determining cyclogenesis in the western ocean basins (Sanders and Gyakum, 1980). Significant SST increases in tropical/equatorial regions are manifest in local enhancements in the convective cloud amounts on short (1-2 days) time scales.

The specification of a time-varying SST to a NWP model would require a corresponding oceanic prediction model. The inclusion of atmospheric forcing influences on SST changes would require an input to the oceanic model from the atmospheric model. The sensitivity of both models to the input from the other must be well understood before truly coupled atmospheric-oceanic models become operational.

A. COUPLING SCHEMES

Three methods of model coupling were described by Elsberry et al. (1982):

1. minimal feedback;
2. non-synchronous coupling; and
3. synchronous coupling.

Minimal feedback (Fig. 1a) is the method used by current operational models. It involves specification of SST at the initial time and no time-dependence of the SST field. Non-synchronous coupling (Fig. 1b) involves SST input from an essentially independent ocean prediction model. Synchronous coupling (Fig. 1c) involves concurrently running oceanic and atmospheric models which provide boundary forcing to each other.

An understanding of the effects of more sophisticated coupling schemes on NWP models is required before these schemes are implemented in operational models. The additional degrees of freedom afforded by the new time dependencies in boundary forcing can possibly degrade model forecast skill, especially that achieved through "tuning" of parameterized processes. Atmospheric model biases may result from biases in the oceanic prediction models or improper coupling between models. A large number of model verification studies will be required to identify these biases with any statistically significant degree of certainty.

B. PREVIOUS STUDIES

Many previous studies have concentrated on long time scale (climatalogical) effects of SST changes on the atmosphere. A review of these studies is contained in Elsberry et al. (1982).

Arpe (1981) examined the effect of artificial SST anomalies on the performance of the ECMWF model. He showed model sensitivity at forecast times of six days and increased cyclogenesis with large-scale positive SST anomalies. Fanelli (1984) examined the effects of observed SST deviations (with respect to the initial conditions) on the NOGAPS model. Clear differences in model behavior were noticed over a 10-day forecast. The model employing the time-dependent SST seemed to show improved skill in predicting mid-latitude maritime storm lifetimes.

III. PROCEDURE

The experimental procedure was similar to that of Ranelli (1984). Two versions of NOGAPS were used in this research. In each of two cases, two NOGAPS integrations to 10 days forecast time were made. The first of the integrations was the control run in which the SST was held constant. In the second integration, designated the SST run, global SST's were updated at every time step (4 minutes) of the model. The model atmospheric responses of each forecast were analyzed for differences. The analysis was restricted to the following fields:

a. surface pressure;
b. sea-surface temperature;
c. surface sensible heat flux;
d. surface latent heat flux;
e. surface total heat flux (includes radiation);
f. convective precipitation; and
g. large-scale precipitation.

The NOGAPS model was made available by Dr. T. Rosmond of the Naval Environmental Prediction Research Facility (NEPRF). The general characteristics of the model were described by Ranelli (1984). During the course of this experiment, major changes were made to NOGAPS. The November 1983 case study was run with a six-layer version of NOGAPS very similar to that used by Ranelli (1984). The April 1984 case was run with the new nine-layer version of NOGAPS. In addition to vertical resolution, the two model versions differed in the method by which diabatic heating was applied. In the earlier version, the diabatic processes were calculated and applied once every 10 model time steps

(40 minutes). The new version also calculates the diabatics every 10 model time steps but applies this heating uniformly at each time step. Consequently, the diabatic effects will be applied smoothly with less shock between the time steps in which diabatic effects are and are not introduced. The effects of time-dependent SST will also be introduced more smoothly in the new NOGAPS. Since additional model levels are included, the coupling between the planetary boundary layer and the free atmosphere should also be enhanced.

Observed sea-surface temperatures were used to simulate the input from an ocean prediction model. The SST analyses are produced twice daily for valid times of 0000 GMT and 1200 GMT. These analyses were used to create fields of 12-hour forward difference SST change. NOGAPS was modified to input these 12-hour forward difference SST changes and apply an incremental portion of the SST change at each time step. This process simulates a synchronous coupling of NOGAPS to a "perfect prog" ocean model.

The NOGAPS initial conditions used for the case studies were identical to those used for the operational forecasts with the same starting times. The case starting times were:

a. 1200 GMT 31 October 1983; and
b. 1200 GMT 21 April 1984.

The model output parameters were analyzed by three methods. Forecast and analyzed vortices were objectively tracked using the Systematic Errors Identification System (SEIS) developed by Brody, et al. (1984) at NEPRF. SEIS is based on the vortex representation system of Williamson (1981). The system tracks vortices in a 900 grid point 'window' in the FNOC 63x63 polar stereographic grid. Separate SEIS runs were required to track Pacific and Atlantic storms. The other model output fields were analyzed in Atlantic and Pacific 'windows' of the FNOC

73x144 spherical grid which extended from 20N to 60N. The SST and control run forecast parameters were differenced (SST-control) and both contour plots and field statistics were used to determine the relationships between the forecast differences and the time-dependent SST.

IV. HEAT FLUX ANALYSIS

The introduction of time-dependent sea-surface temperatures into the NOGAPS model results in immediate changes in the surface fluxes of sensible and latent heat. These fluxes in NOGAPS are parameterized according to Deardorff (1972). Because the PBL and convective parameterization schemes in NOGAPS are intimately coupled, the changes in air-sea fluxes may change the diabatic forcing throughout the troposphere.

A. SEA-SURFACE TEMPERATURE CHANGES

In both the November and April cases, significant SST changes evolved during the 10-day forecast period. The SST difference field (day 10 - initial conditions) for the November case is shown in Fig. 2. Large-scale negative SST changes are evident in the western Pacific Ocean, Sea of Okhotsk, eastern Pacific Ocean, and mid-Atlantic Ocean. There were small areas of weak positive SST change to the west of the British Isles and to the east of the northeastern United States. The SST difference fields for the April case are shown in Fig. 3. While both positive and negative SST changes are shown, the overall mean SST difference is positive. Large positive differences are found in the Sea of Japan, Yellow Sea, eastern Pacific and western Atlantic Oceans. Negative differences (decreasing SST with time) occur in the western Pacific (east of Japan) and north Atlantic (south of Greenland). The evolution of the field mean SST differences for each ocean basin in both cases is shown in Fig. 4. The 10-day trends in the mean SST differences are essentially linear. Correlation coefficients of

linear regressions on the field-mean SST differences were between 0.86 and 0.99. Some of this trend is due to the actual SST observations. In addition, the TOPS-EOTS forecast/analysis scheme includes a time-dependent effect in the first guess and a reversion to climatology in data-sparse areas. Each of these effects will also contribute to a general trend.

B. SURFACE HEAT FLUX CHANGES

As in Panelli (1984), the surface heat fluxes were responsive to the SST changes. However, the spatial patterns of heat flux differences were not always related directly to the patterns of SST difference. The heat flux difference patterns often took the form of couplets of positive and negative differences.

1. Sensible Heat Flux

The field mean heat flux differences did show trends similar to the SST differences. The 12-hour fields of sensible heat flux differences were extremely noisy. Features in the difference fields were rarely stable for 48 hours. The largest differences, both positive and negative, were observed in the western ocean basins in the November case and in the Pacific Ocean south of 30 N for the April case.

The development of the mean sensible heat flux differences is shown in Figs. 5 through 8. While the field-mean differences reach 5-20 percent of the control forecast mean sensible heat flux, peak values in the difference fields exceed 50 percent of peak values in the control forecast fields. Peak differences exceed the mean control fluxes by factors of 2-15. Correlation coefficients of linear regressions of the field-mean differences were from 0.04 to 0.56.

2. Latent Heat Flux

The latent heat flux difference fields showed less noise and more stability than those of sensible heat flux. A direct correlation of the latent flux difference fields and SST difference fields was not obvious. Representative latent heat flux difference fields are shown in Fig. 9. In the November case, strong positive-negative couplets developed in the western Atlantic region. The Pacific Ocean areas south of 30 N exhibited the largest differences in the April case. Analysis of the field statistics (Figs. 10 through 13) shows mean differences reaching 5-12 percent of the control means. Peak values in the difference fields reach 25-75 percent of the peak values of the corresponding control latent heat flux fields and exceed field-mean fluxes in the control run by factors of 2-6. Linear regression of the field-means produced correlation coefficients of 0.75-0.88 in the November case and only 0.22-0.60 in the April case. The differences in latent heat fluxes after 10 days during November are at least 10 times as large as the differences in sensible heat fluxes, and represent considerable reductions in evaporation over the entire field.

3. Total Heat Flux

NOGAPS total heat flux includes the sensible and latent fluxes plus the net radiative flux at the surface. The radiation is affected by model cloudiness. Fields of total heat flux difference tend to be correlated with fields of latent heat flux difference. Field statistics (Figs. 14 through 17) showed mean differences of 8-20 percent over the 10-day forecast periods. Peak differences at specific times were 40-100 percent of the control peak fluxes and exceeded control field-means by factors of 2-10. Linear regression of the field-means produced correlation coefficients of

0.44-0.94 in the November case and 0.12-0.46 in the April case. Especially in the November case, these differences after 10 days represent significant changes in the surface heat budget terms which would be used to drive the ocean model.

C. SUMMARY

The introduction of time-dependent sea-surface temperatures resulted in significant field-mean sensible, latent and total heat flux differences of up to 20 percent over 10-day forecast periods. Maxima in the flux differences between the SST and control runs after 10 days were of the same order of magnitude as peak values in the control flux fields. Thus, the surface fluxes at individual points may differ significantly from the control run when time-dependent SST's are specified. Stable features in the difference fields of latent and total heat flux were observed to intensify and move consistently during the second half of the forecast period. The largest changes were noted in the western Atlantic in the November case and in the Pacific (south of 30 N) for the April case.

The forecast differences in heat fluxes are of such magnitude that they can be expected to change the nature of the atmospheric (and oceanic) forecast at some future time. Local changes in the heat fluxes could also be expected to seriously affect model-derived forecasts, such as those produced by model-output statistics and systems similar to the Navy Operational Local Atmospheric Prediction System (NOLAPS), since these products depend on the predicted surface fluxes.

The changes in the surface heat fluxes were greater than those observed by Ranelli (1984). Three key differences in the experiment procedures account for the differences in

heat flux observations. A full 10 days of SST change were input vice 7 days during the Panelli study. The application of diabatic heating by the new NOGAPS increased the effects of a time-dependent SST as did the updating of SST every 4 minutes (vice 12 hours) of forecast time.

V. PRECIPITATION ANALYSIS

Changes in the surface heat fluxes induced by time-dependent sea-surface temperatures can be expected to affect convective and large-scale precipitation forecasts. A study by Bosse (1984) showed that surface heat fluxes could be related to NOGAPS large-scale precipitation fields through layer cloud instability.

A. CUMULUS PRECIPITATION

The development of the cumulus precipitation difference fields during the 10-day forecasts is shown in Figs. 18 through 21. Over both the North Pacicic and North Atlantic, there are 25 to 50 percent decreases in mean cumulus precipitation during the November forecast. In the April forecast, mean cumulus precipitation over the Pacific decreased almost 15 percent while cumulus precipitation over the Atlantic increased 20 percent. Peak difference values exceeded 100 percent of peak at some time during each of the forecasts. The decrease in cumulus precipitation during the November period seems logical in view of the decreasing mean sea-surface temperatures and latent heat fluxes. However, the magnitude of the changes is surprisingly large. Correlation coefficients of 0.74 were obtained in linear regression of both the Atlantic and Pacific mean cumulus precipitation differences. The magnitudes of the SST and latent heat flux field-mean differences were much less in the April case than in the November case. The variance of both mean SST change and mean flux change was greater in the April case than in the November case due to the presence of areas of strong positive and negative SST change in both

ocean basins. This may explain the less consistent changes in cumulus precipitation during the April forecast. Correlation coefficients for the linear regression of the mean cumulus differences during the April period were 0.61 in the Pacific and 0.007 in the Atlantic.

B. LARGE-SCALE PRECIPITATION

The development of the large-scale precipitation difference fields is shown in Figs. 22 through 25. Mean differences of large-scale precipitation are less than 10 percent except for the April Atlantic at the end of the forecast period. Peak differences range from 75 to 100 percent of peak control values.

C. SUMMARY

Significant mean and peak precipitation differences were observed during the 10-day forecasts. As with the heat flux differences, these changes in model precipitation grow with time. Long range model-derived products such as model-output statistics will be affected by these differences.

VI. ANALYSIS OF STORM TRACKS

The SEIS program (Brody, et al., 1984) was used to objectively analyze the position, size, shape and amplitude of low pressure systems in the control and SST forecasts and the analyses. The analysis was performed on surface pressure only.

The SEIS storm parameters are defined in a manner similar to that of Williamson (1981). Amplitude is the difference between the storm central pressure and the latitudinally-averaged surface pressure. Radius is the size of the storm expressed in terms of the spacing of the FNOC Northern Hemisphere polar stereographic grid. Ellipticity is the square root of the ratio of the semi-major and semi-minor axes of the ellipse which best fits the analyzed storm shape. Angle is the angle between the x axis and the storm ellipse major axis, measured counterclockwise from the x axis.

In the SEIS program, the forecast low pressure systems are analyzed first, then low pressure systems in the analyses, then forecast and analyzed systems are matched according to set criteria. The nominal SEIS matching criteria are plus or minus 2.5 grid points in both the x and y directions and plus or minus 12 hours in time. SEIS is routinely used to evaluate 60 hour forecasts and the matching criteria are optimized for this period. As a result, the vortex tracking and description portions of SEIS perform satisfactorily throughout the 10-day forecasts, but the automatic matching portion of SEIS becomes ineffective after five days. This is primarily a function of the overly restrictive time matching criteria. Inspection of the SEIS output indicated that several good storm track matches in

the 5-10 day portion of the forecast period could be made if the time matching criteria were increased to plus or minus 48 hours. Manual matching with the standard distance criteria and 48 hour time criteria was used in the 5-10 day portion of the forecasts.

Labels were assigned to the matched storm tracks for discussion and reference purposes. The storm labels consist of 3 characters. The first character is the first letter of the forecast month (N for November, A for April); the second character is the first letter of the ocean basin (A for Atlantic, P for Pacific); and the third character is a numeral assigned on the basis of chronological order of storm identification within a particular forecast and ocean basin.

A. STORMS DURING NOVEMBER

The November control and SST forecasts were made with the six-level version of NOGAPS. A total of 15 storms with lifetimes greater than 36 hours were tracked in the surface pressure analyses. Fifteen storms were present in the control forecast while 16 were tracked in the SST forecast. Matches were obtained for eight of the 15 analyzed storm tracks.

Relatively minor differences between the control and SST forecast storm positions and parameters were noted. These differences grew with time. The tracks for storm NA5, which showed the largest track and parameter differences, are shown in Fig. 26. This storm was first identified at 72 hours in the analyses and at 96 hours in both forecasts. The analysis and control forecast storm lifetimes of 120 hours are identical while the SST storm lifetime was 24 hours longer. The forecast storm tracks diverge after the third forecast but remain almost parallel. The control run

storm remains quasi-stationary north of Great Britain four days after first detection, while the SST run storm stalls for only 12 hours in the same region and then proceeds to the northeast. The cyclogenesis and early storm tracks of NA5 are in the region of maximum SST change, but the late tracks and cyclolysis positions are in the region of minimum SST change. The SEIS parameters for storm NA5 are shown in Fig. 27. The forecast amplitude and period of maximum radius lag the analyzed parameters by 48 to 60 hours. The control run was more accurate than the SST run in this particular case, although the differences are much smaller than the departures of the forecasts from the analyses. The NA5 forecast was the only one of the eight November storms for which one forecast could be judged more accurate than the other. The descriptions, tracks and parameters for the other seven November storms are contained in Appendix A.

B. STORMS DURING APRIL

The April control and SST forecasts were made with the nine-layer version of NOGAPS. A total of 11 storms with lifetimes greater than or equal to 36 hours were tracked in the surface pressure analyses. Fourteen were tracked in the control forecasts, while 15 were present in the SST forecasts. Matches were obtained for seven analyzed storm tracks. Significant differences between control and SST forecast tracks and parameters were found for three of the seven matched tracks. Those matched tracks with significant differences are discussed here. The remainder of the April storm tracks are discussed in Appendix A.

1. Storm AA3

The tracks and SEIS parameters for storm AA3 are shown in Figs. 28 and 29. This storm was first detected in

the analyses at 84 hours and was forecast only by the SST run at 108 hours. The forecast storm was weaker (5 mb) and shorter-lived (36 vice 168 hours) than the actual storm, but the cyclogenesis position and initial track were well predicted. This was the only case for which only one of the forecast models predicted a matched storm track when the other forecast model did not. The cyclogenesis position was to the west of, and the storm track over, an area of maximum positive SST change. The SST forecast was clearly superior to the control run in this case, especially considering that the storm developed around the fourth day of the forecast.

2. Storm AA4

The tracks and SEIS parameters for storm AA4 are shown in Figs. 30 and 31. Storm AA4 was forecast by both the control and SST runs at 120 hours and was first detected in the analysis 12 hours later. The cyclogenesis position was in an area of maximum positive SST change (1.2 C). Both forecasts overestimated the actual storm lifetime of 72 hours by 48 hours. The forecast tracks were similar until the sixth forecast (third day after formation), when the SST storm began erratic movement. The forecast SEIS parameters in Fig. 31 are similar, with significant differences in radius and angle at the second forecast period and radius and ellipticity at the eighth forecast period. The control track forecast for AA4 was very slightly more accurate than the SST track forecast during the first three days. The differences between the forecasts again are much less than the departures of each forecast from the analysis.

3. Storm AP3

The tracks and SEIS parameters for storm AP3 are shown in Figs. 32 and 33. Cyclogenesis occurred at 60 hours in both forecasts and the analysis. The cyclogenesis and

tracks were in an area of positive SST change (0.4-0.8 C). The control run forecast a weak storm with a lifetime of only 12 hours whereas the SST run predicted a lifetime of 60 hours. Since the analyzed storm lifetime was 48 hours, the SST run more accurately predicted the storm lifetime and track in this case. The amplitude (Fig. 33) of this relatively weak storm was forecast rather accurately in the SST run.

C. SUMMARY

Significant differences in the forecast tracks and SEIS parameters were noted in four of the 15 matched storm tracks. The control run was more accurate in two of the cases, correctly forecasting November cyclolysis when the SST run did not and more closely matching an April storm track when the SST run exhibited erratic movement. The SST run was more accurate in two April cases, forecasting an analyzed cyclogenesis which the control run did not and maintaining a storm in which the control run forecast premature cyclolysis. The different method of applying the diabatic forcing and the increased vertical resolution of the three-level NOGAPS used in the April runs made direct comparisons of the November and April forecasts difficult. The results were very encouraging. It appeared that the model was sensitive to the effects of the [illegible] that this sensitivity translated into [illegible] in two cases.

VII. CONCLUSIONS

The introduction of time-dependent sea-surface temperatures into the NOGAPS model resulted in significant changes in mean and peak surface heat fluxes and precipitation. Forecasts which use these fields directly, such as model-output statistics, TOPS and NOLAPS-type models, may benefit from the incorporation of time-dependent sea-surface temperatures.

Differences between the control and SST forecast storm tracks and SEIS parameters were significant in 4 of the 15 matched storms. The April SST run, which utilized the nine-level NOGAPS model, correctly predicted cyclogenesis and cyclone maintenance for two cases in which the control run did not. The control run more accurately predicted a November cyclolysis event and one April storm track. Only minor differences in forecast positions and SEIS parameters were noted in the other 11 matched storms. Differences in the SEIS parameters were evident before those in storm position. The new nine-level NOGAPS, with sophisticatic application of diabatic forcing, seems sensitive to the effects of time-dependent SST in a way which improves the accuracy of some forecasts.

This study was limited in its application and results. Further studies on the response of atmospheric prediction models to time-dependent SST will be required to make statistically significant inferences about the effects of such boundary conditions on the quality of the numerical forecasts. Additional case studies with the analyses extended to cover the tropical and Southern Hemisphere ocean areas should be conducted. Additional model variables, such as cloudiness, PBL thickness and static energy and diabatic

and cumulus heating should be analyzed. Further attempts should be made to verify the heat flux and precipitation forecasts of models which incorporate time-dependent SST to determine model sensitivity and biases. The effect of model output changes on proposed long range model-output statistics and other model-derived forecasts should also be evaluated.

APPENDIX A
STORM TRACK DATA

The 11 forecast storm tracks which were judged to show less significant differences are discussed in this appendix. In general, storms which were present in the forecast initial conditions or developed early in the forecast period did not develop significant differences between the control and SST forecasts.

A. STORMS DURING NOVEMBER

1. Storm NA1

The tracks and SEIS parameters for storm NA1 are shown in Figs. 34 and 35. This storm was present in the initial conditions of both forecasts. Only minor differences between the SST and control forecast parameters develop after six to eight 12-hour forecasts. Both forecast storms moved too slowly after 24 hours and persisted longer than the analyzed storm.

2. Storm NA2

The tracks and parameters for storm NA2 are shown in Figs. 36 and 37. In this case both forecasts accurately predicted storm lifetime while moving the storm too quickly and in a more zonal path than was analyzed. Minor differences in only two parameters, position and angle, can be seen at the sixth forecast period.

3. Storm NA3

The tracks and parameters for storm NA3 are shown in Figs. 38 and 39. This storm formed at 72 hours into the

240-hour forecasts. Minor differences in the forecast storm parameters are evident from the time of cyclogenesis. Both forecasts underestimated storm lifetime. The analyzed storm moved erratically and regenerated after the tenth forecast period. Neither model was able to predict the storm regeneration.

4. Storm NA4

The tracks and parameters for storm NA4 are shown in Figs. 40 and 41. This storm formed at 72 hours. While the control and SST forecast parameters are similar, the control storm lifetime was 36 hours greater than that of the SST forecast. The analysis and both forecast tracks were erratic.

5. Storm NP1

The tracks and parameters for storm NP1 are shown in Figs. 42 and 43. This Aleutian low was present in the initial condition of both forecasts and persisted for 7 days in each case. A rather extreme southeastward deflection in the analysis occurred between the third and fourth from the end positions. Differences in the SEIS forecast parameters are apparent after the seventh through ninth forecasts. Only minor forecast storm position differences are evident.

6. Storm NP2

The tracks and parameters for storm NP2 are shown in Figs. 44 and 45. This storm formed at 24 hours into the 240-hour forecast period. Both forecasts underestimate storm lifetime. No differences in the forecast storm tracks, and only minor differences in the forecast SEIS parameters, were noted.

7. Storm NP3

The tracks and parameters of storm NP3 are shown in Figs. 46 and 47. Storm NP3 was the extratropical transition of a tropical cyclone which was not analyzed until 48 hours into the forecast. SEIS did not track this vortex until 132 hours because the storm size was less than 2 grid lengths. Both forecasts predict cyclogenesis in the area of the actual extratropical transition approximately 48 hours before it actually occurred.

B. STORMS DURING APRIL

1. Storm AA1

The tracks and parameters for storm AA1 are shown in Figs. 48 and 49. This high latitude storm was present in the initial conditions of both forecasts. Despite the 120 to 132 hour forecast storm lifetime, only minor differences in the forecast positions and parameters are noted. The analyzed and forecast storm tracks are roughly parallel to the climatic ice edge.

2. Storm AA2

The tracks and parameters for storm AA2 are shown in Figs. 50 and 51. This storm formed 12 hours into the forecast period. Both forecasts seriously overestimated the analyzed storm lifetime by of 36 hours by 72 to 84 hours.

3. Storm AP1

The tracks and parameters for storm AP1 are shown in Figs. 52 and 53. This storm formed 24 hours into the forecast period. Both forecasts moved the storm too far inland and overestimated the actual lifetime of 24 hours by 48 hours. One would not expect significant effects due to time-dependent SST on the time scale of these forecasts.

4. Storm AP2

The tracks and parameters for storm AP2 are shown in Figs. 54 and 55. This storm formed at 48 hours in the analysis and both forecasts. Both forecasts underestimated the actual storm lifetime of 168 hours by 96 hours. As shown by the radius in Fig. 55, this was a rather small storm. Although the radius was well predicted for 6-7 12-hour periods, the amplitude was too small and the SEIS could no longer track the storm.

APPENDIX B
FIGURES

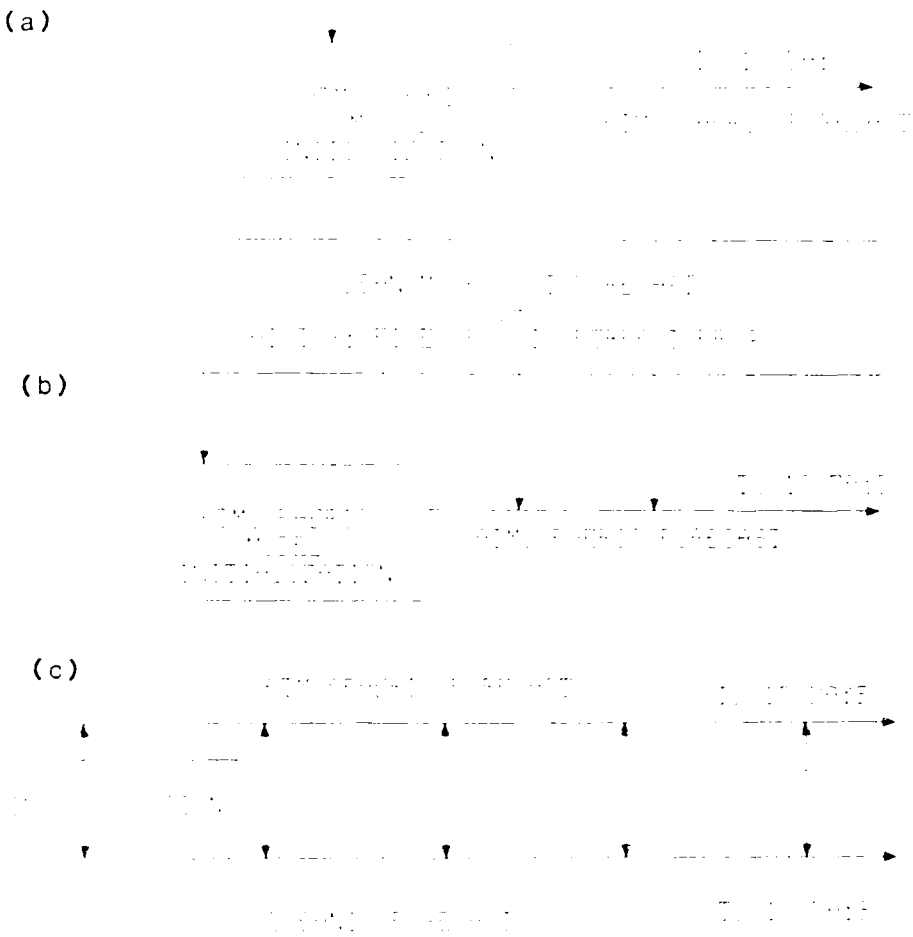

1. Methods for coupling atmospheric and oceanic models (a) minimal feedback, (b) non-synchronous and (c) synchronous.

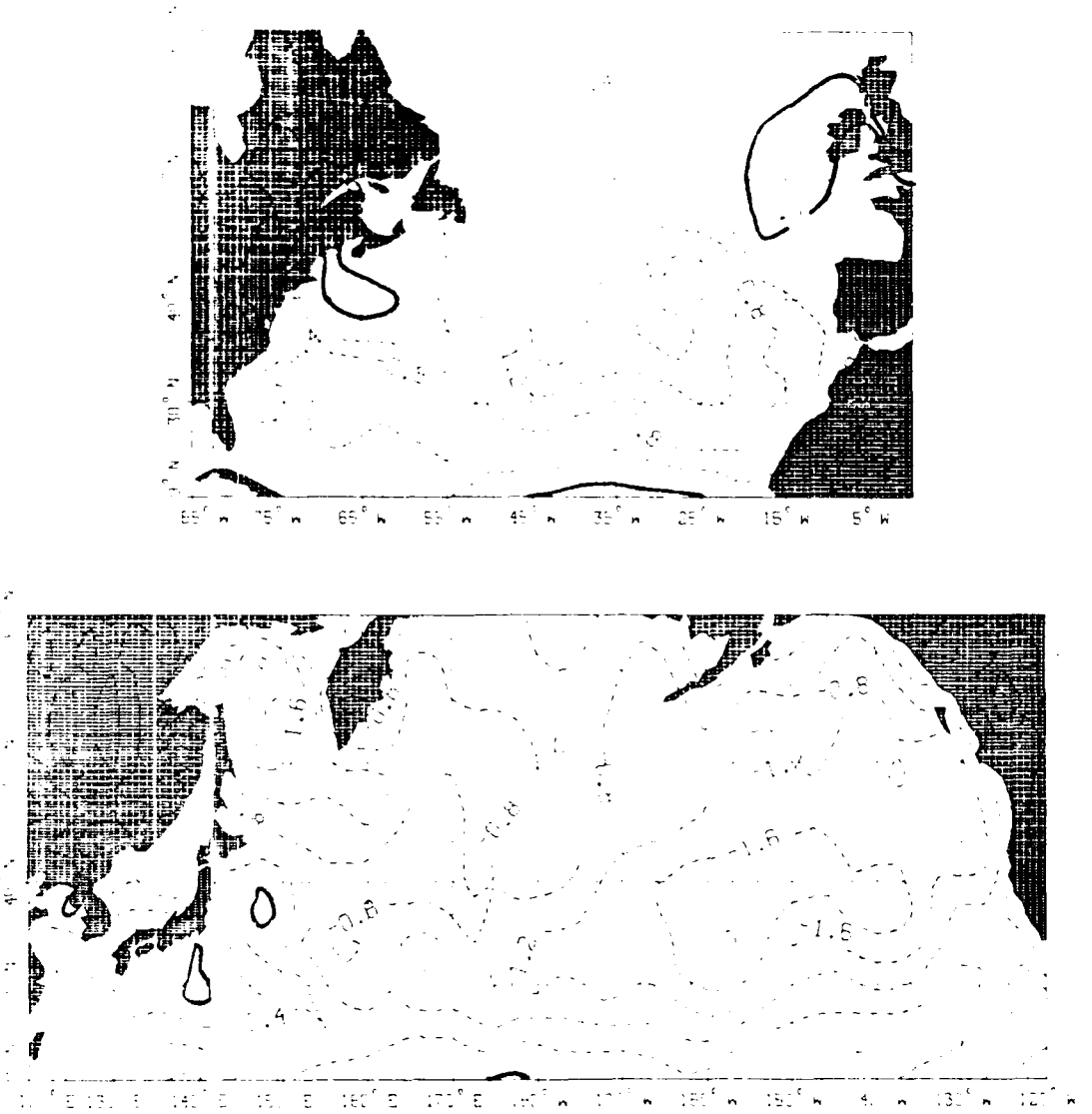

2. The difference between the SST field at day 10 of the model run and the initial SST field for the November case. Contour interval is 0.4 C. Thin solid lines are higher SST, thick solid line is no change and dashed lines are lower SST.

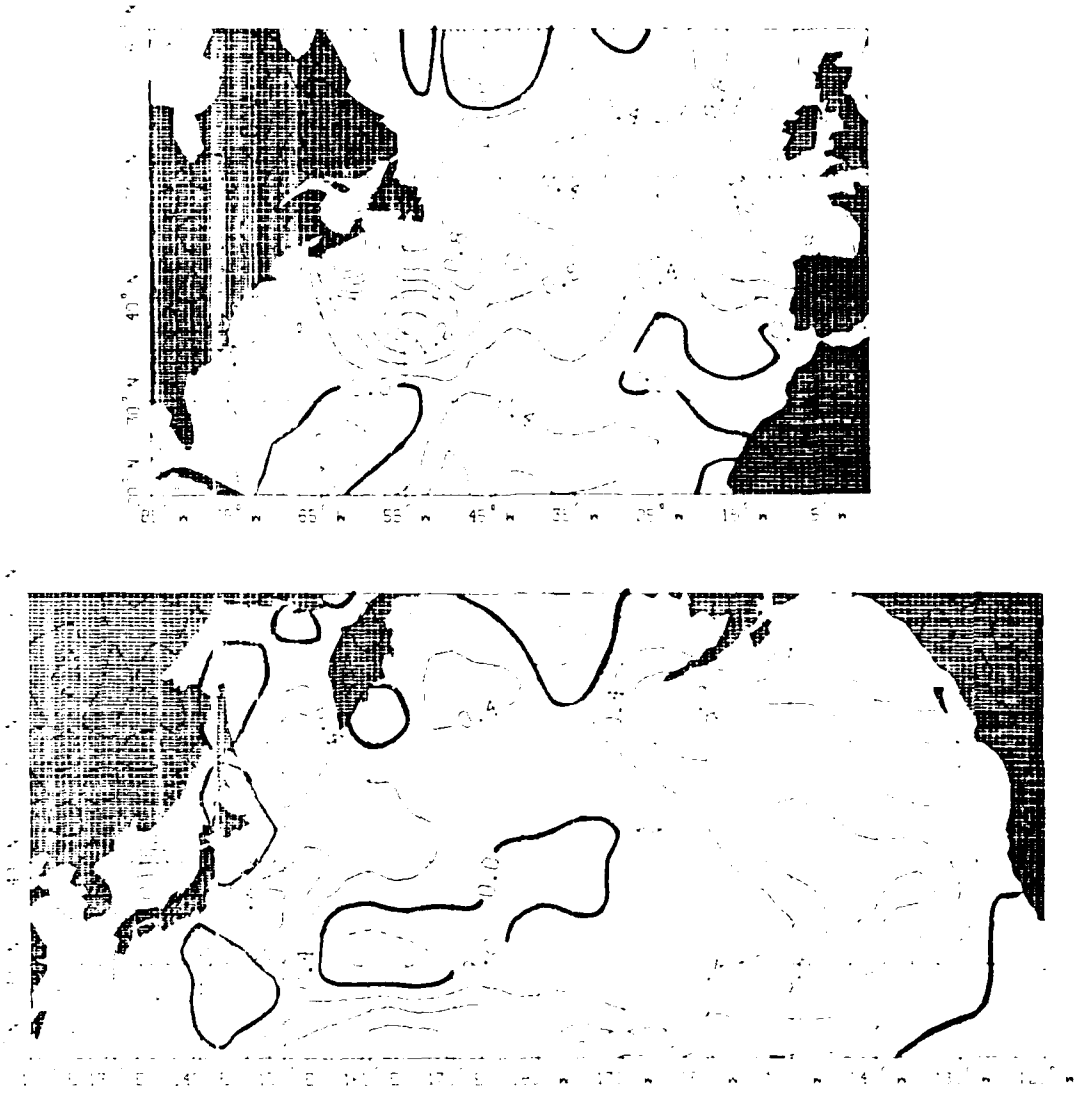

3. The difference between the SST field at day 10 of the model run and the initial SST field for the April case. Contour interval is 0.4 C. Thin solid lines are higher SST, thick solid line is no change and dashed lines are lower SST.

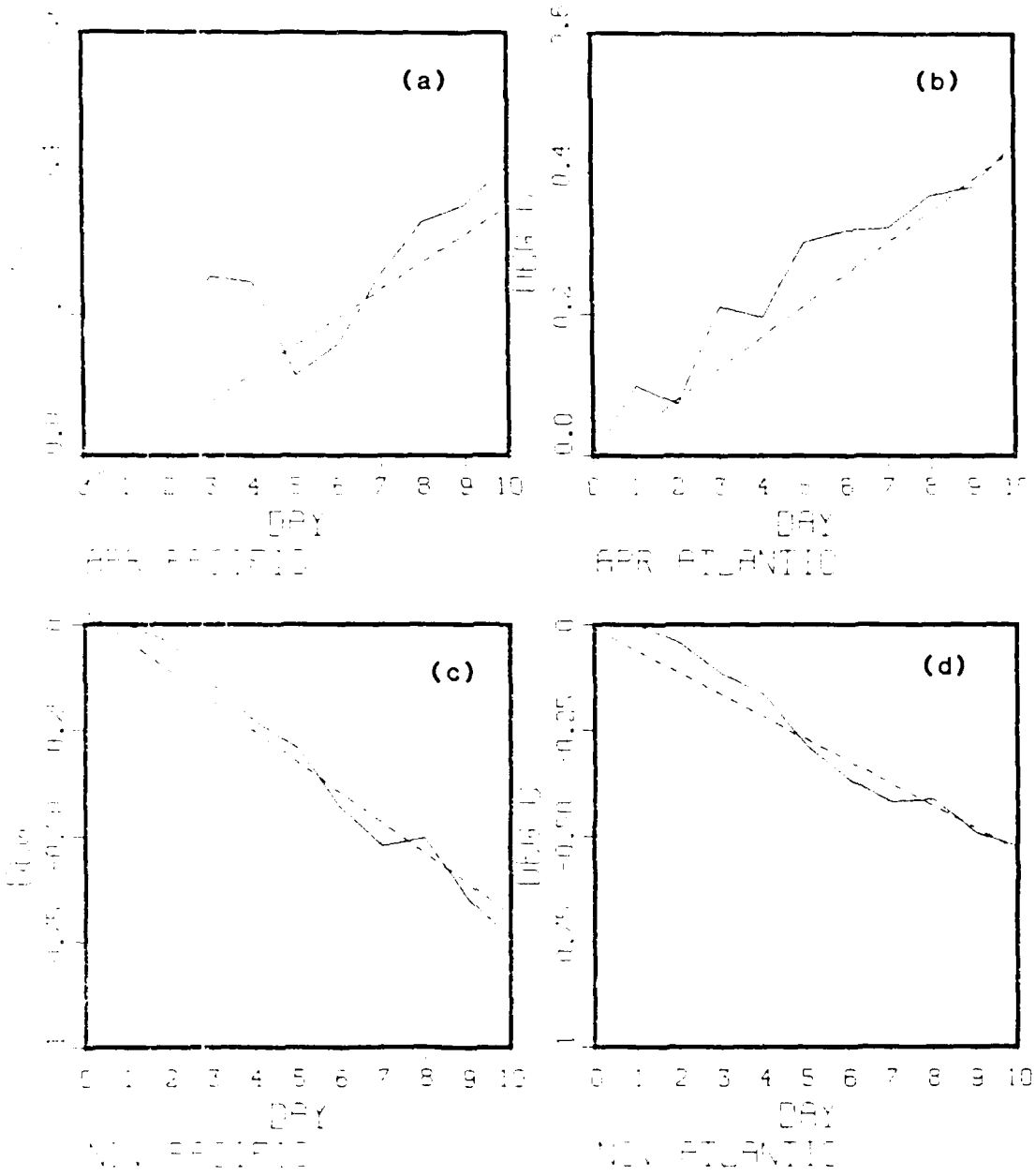

4. Field-mean SST differences (C) during April in (a) Pacific and (b) Atlantic and during November in (c) Pacific and (d) Atlantic. Dashed lines are linear regression of mean SST difference.

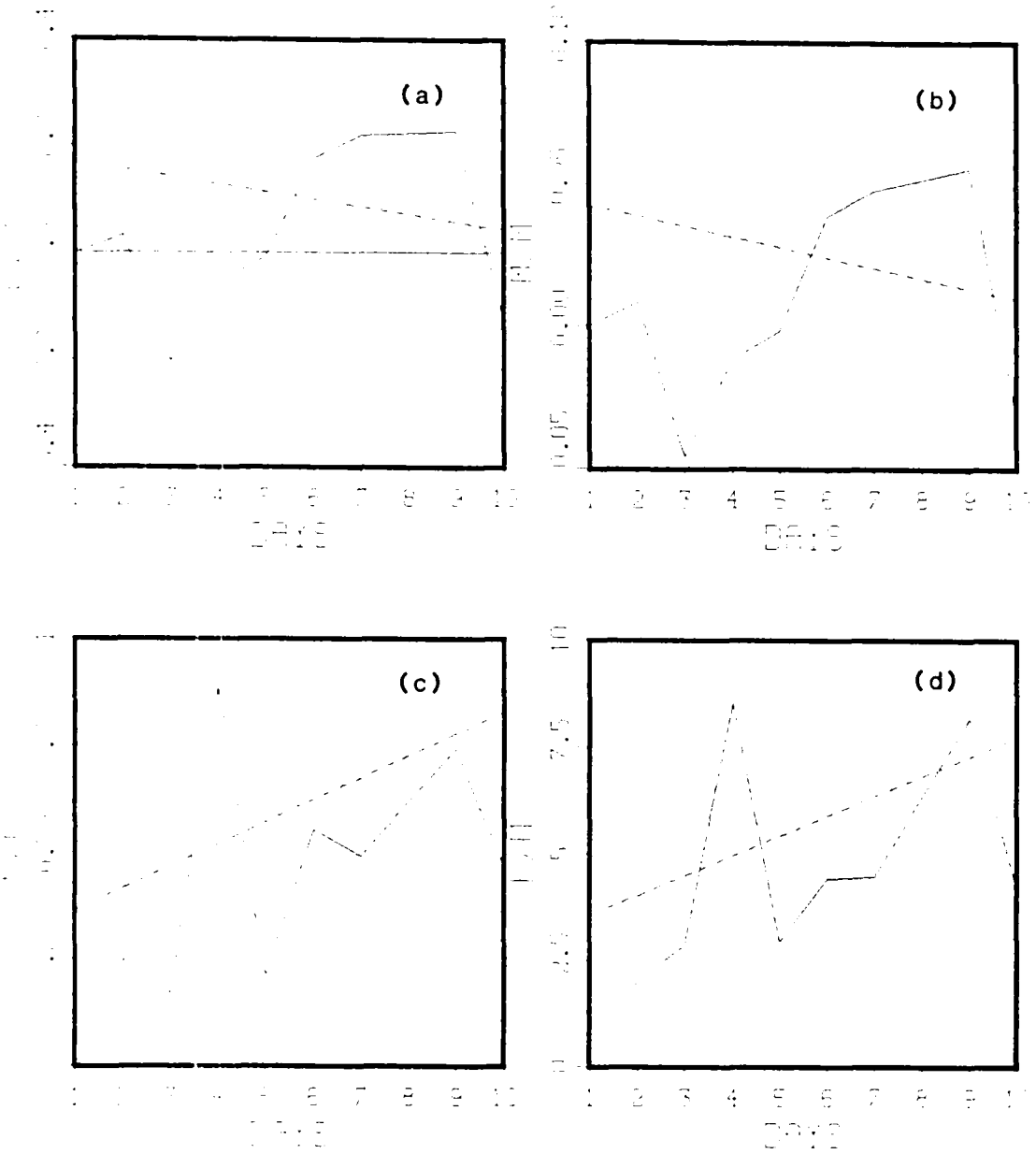

5. Field statistics for sensible heat flux during November for the Atlantic region. (a) Field-mean difference in gm-cal/cm²-h. (b) Ratio of field-mean difference to field-mean control. (c) Ratio of peak difference to peak control. (d) Ratio of peak difference to mean control.

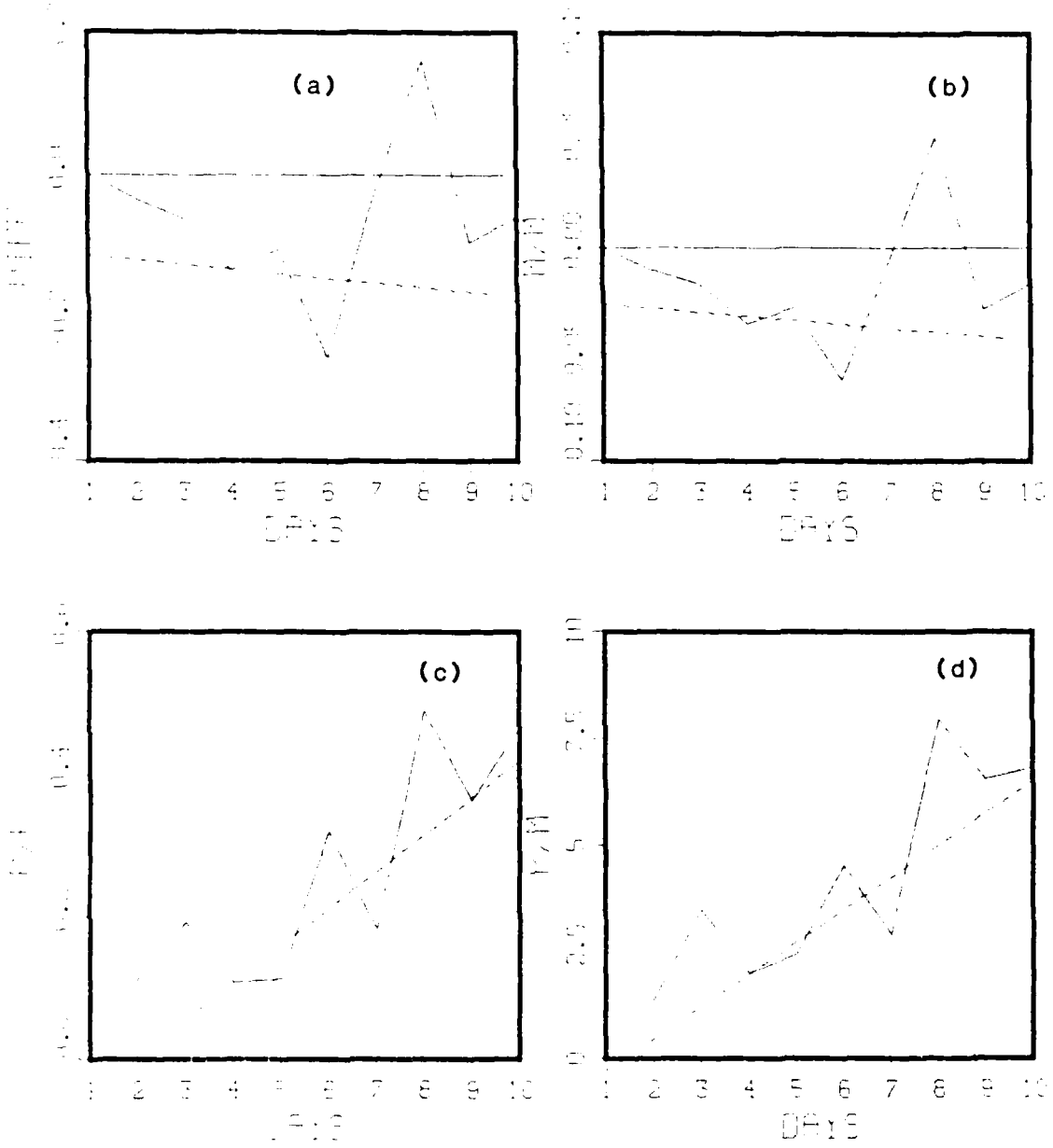

6. Similar to Fig. 5, except for Pacific region.

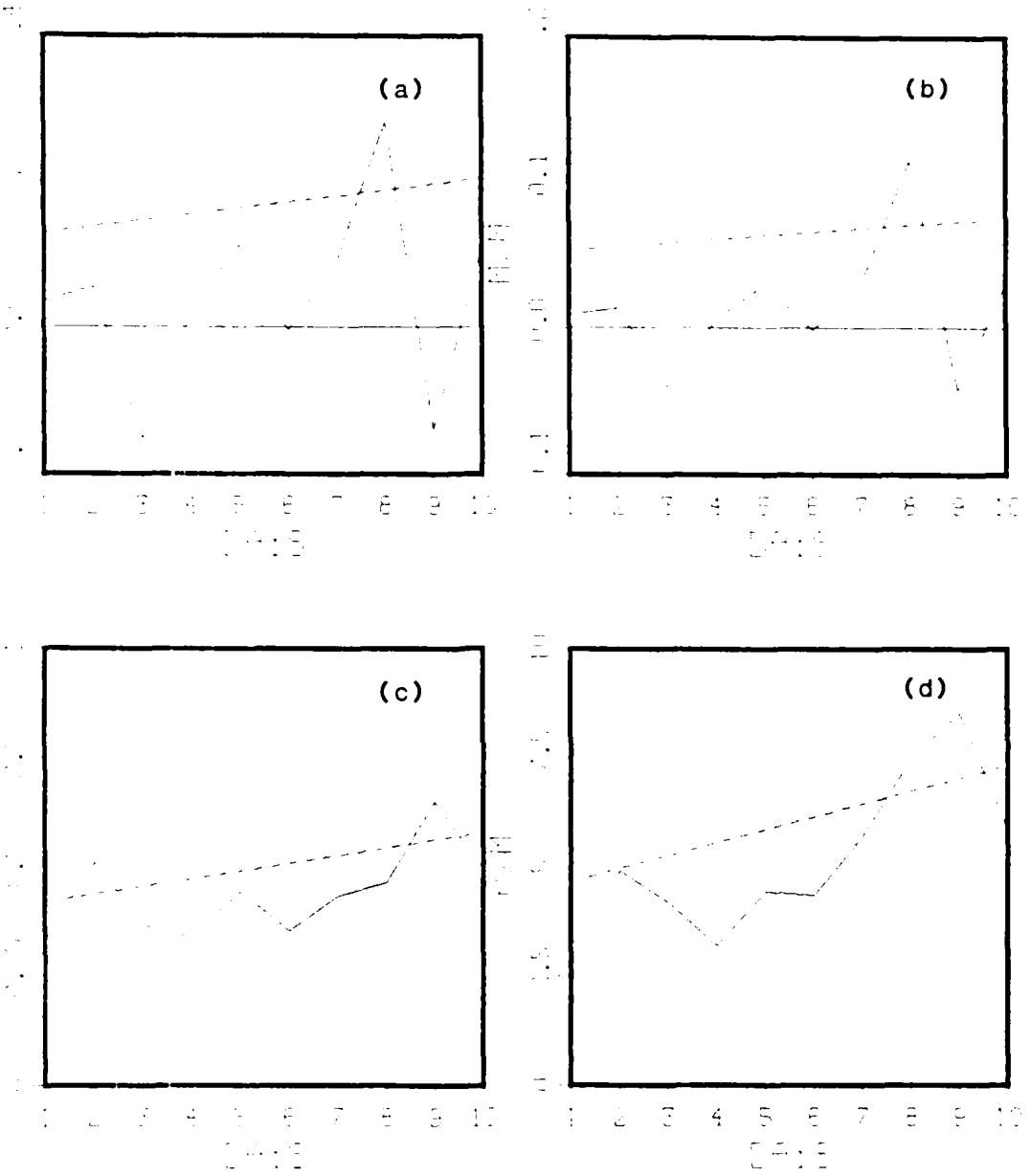

7. Similar to Fig. 5, except for Atlantic during April.

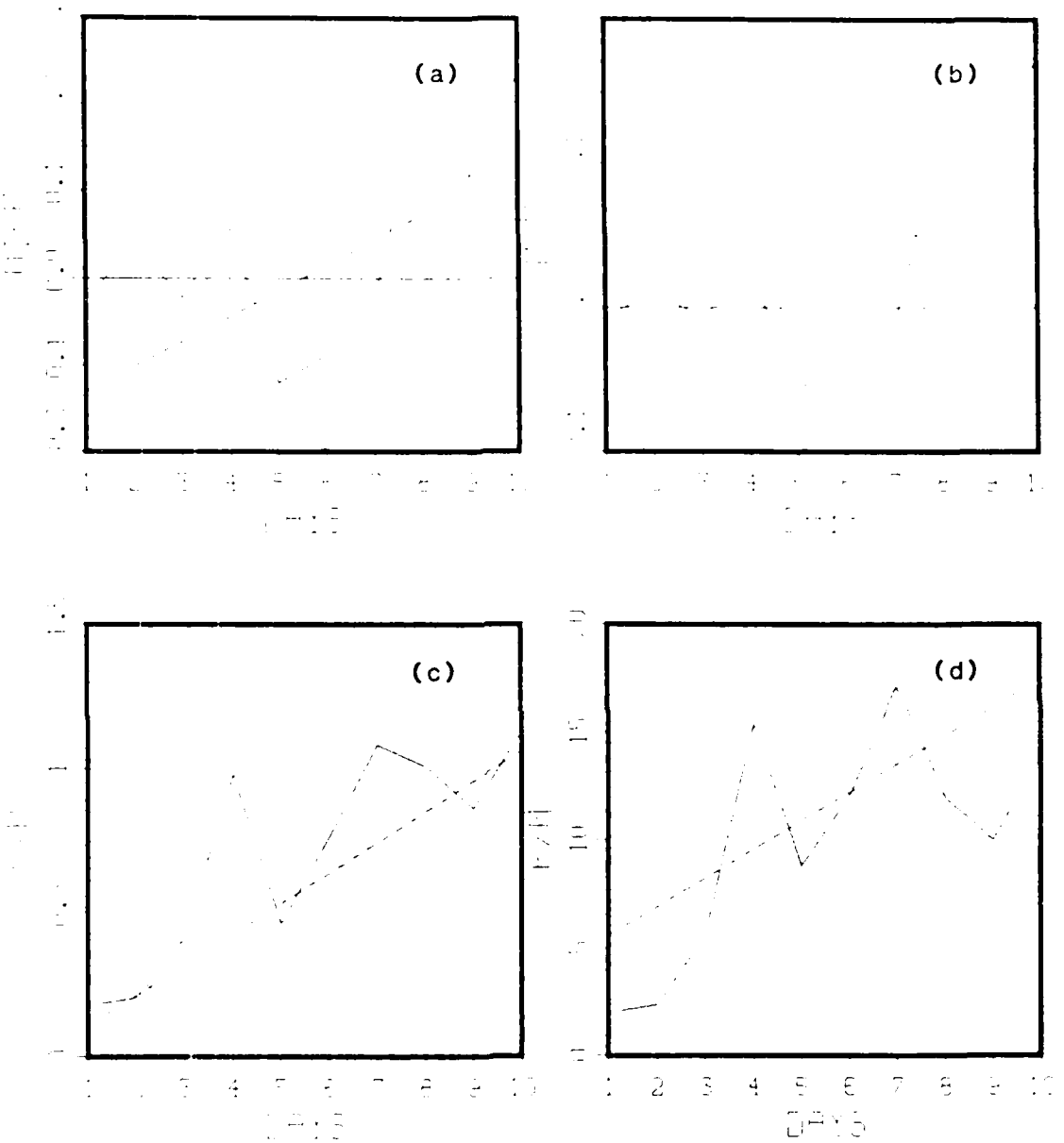

8. Similar to Fig. 7, except for Pacific.

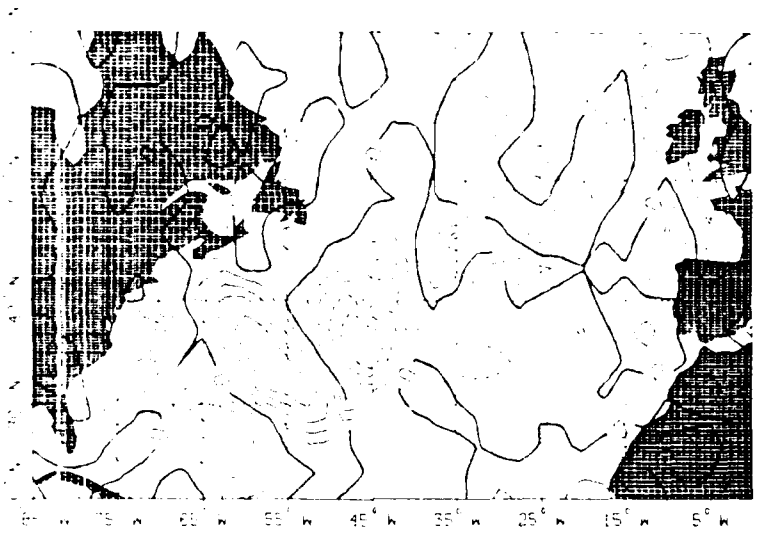

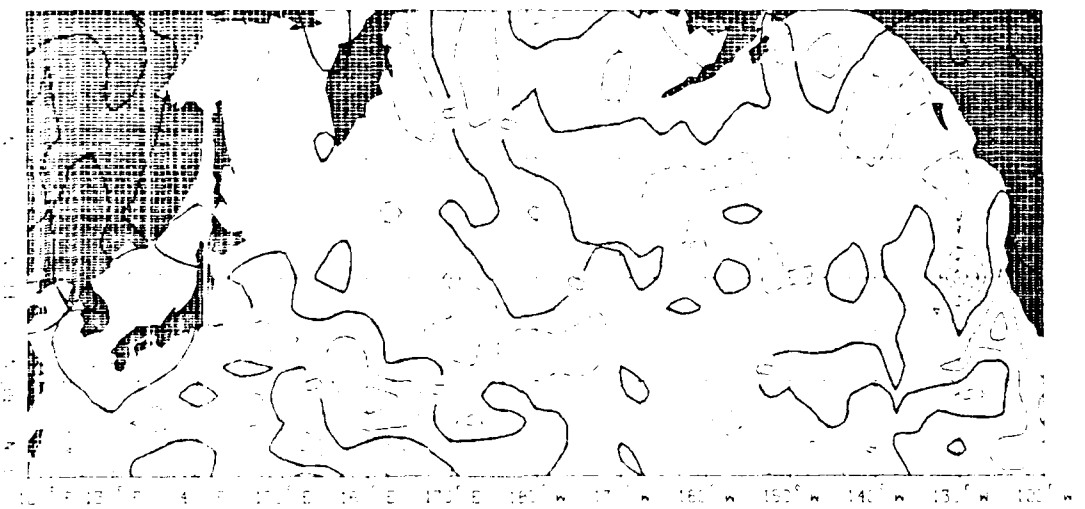

9. The difference between the latent heat flux fields of the SST and control runs at day 10 for the November case. Contour interval 5 gm-cal/cm²-h. Thin solid lines are higher LHF, thick solid line is no change and dashed lines are lower LHF.

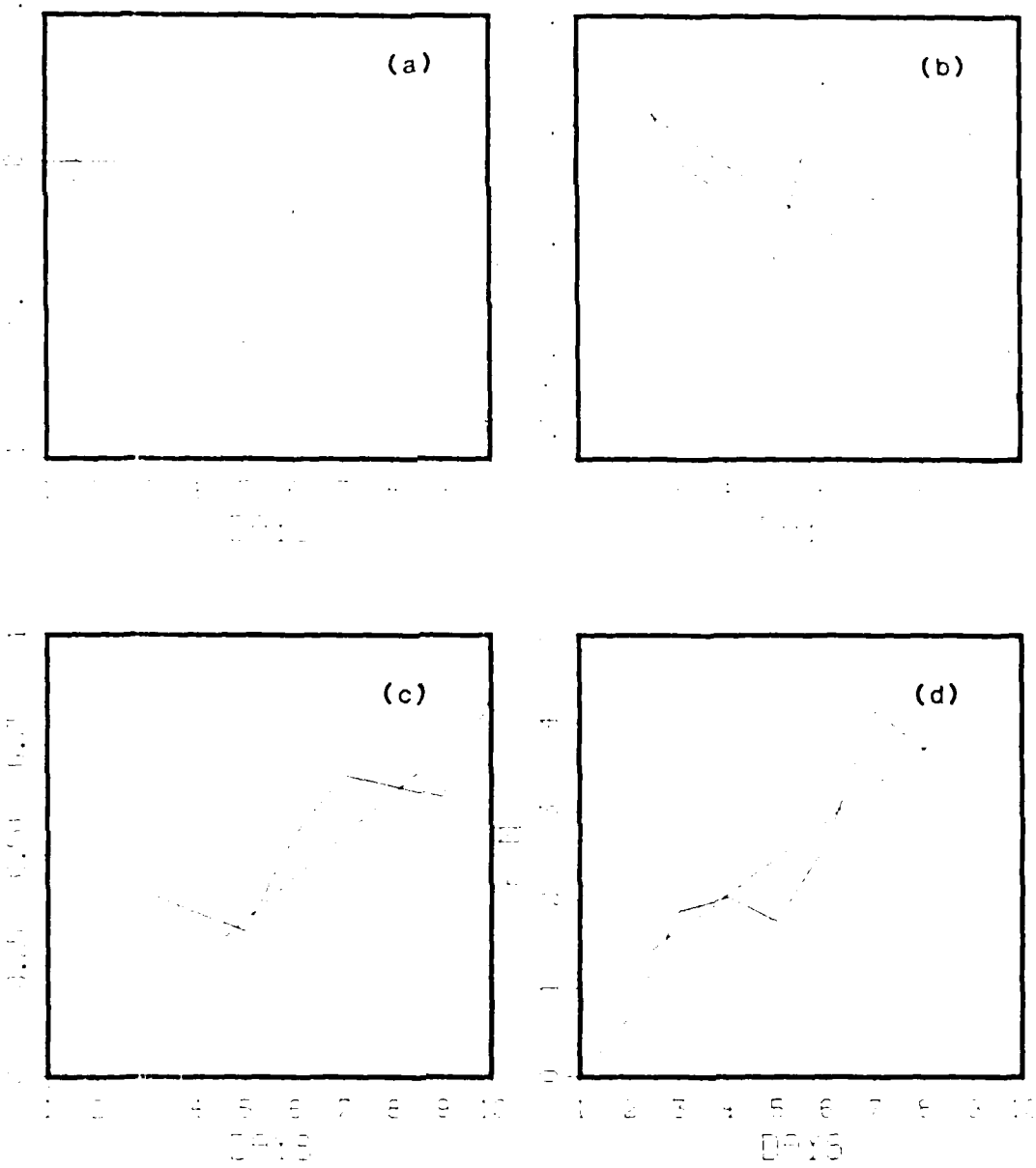

19. Field statistics for latent heat flux during November in in the Atlantic region. (a) Field-mean difference in gm-cal/cm²-h. (b) Ratio of field-mean difference to field-mean control. (c) Ratio of peak difference to peak control. (d) Ratio of peak difference to mean control.

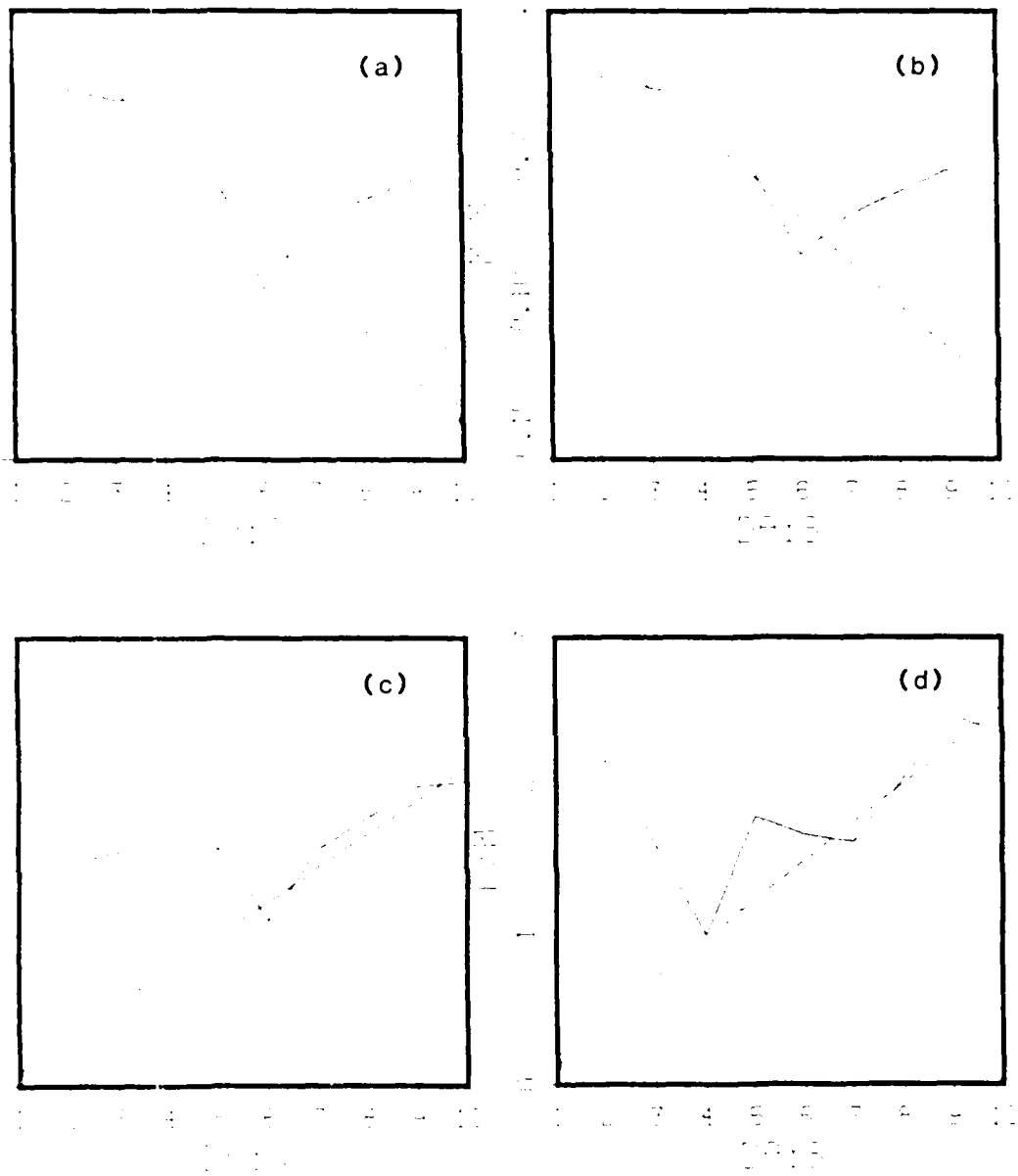

11. Similar to Fig. 10, except in Pacific region.

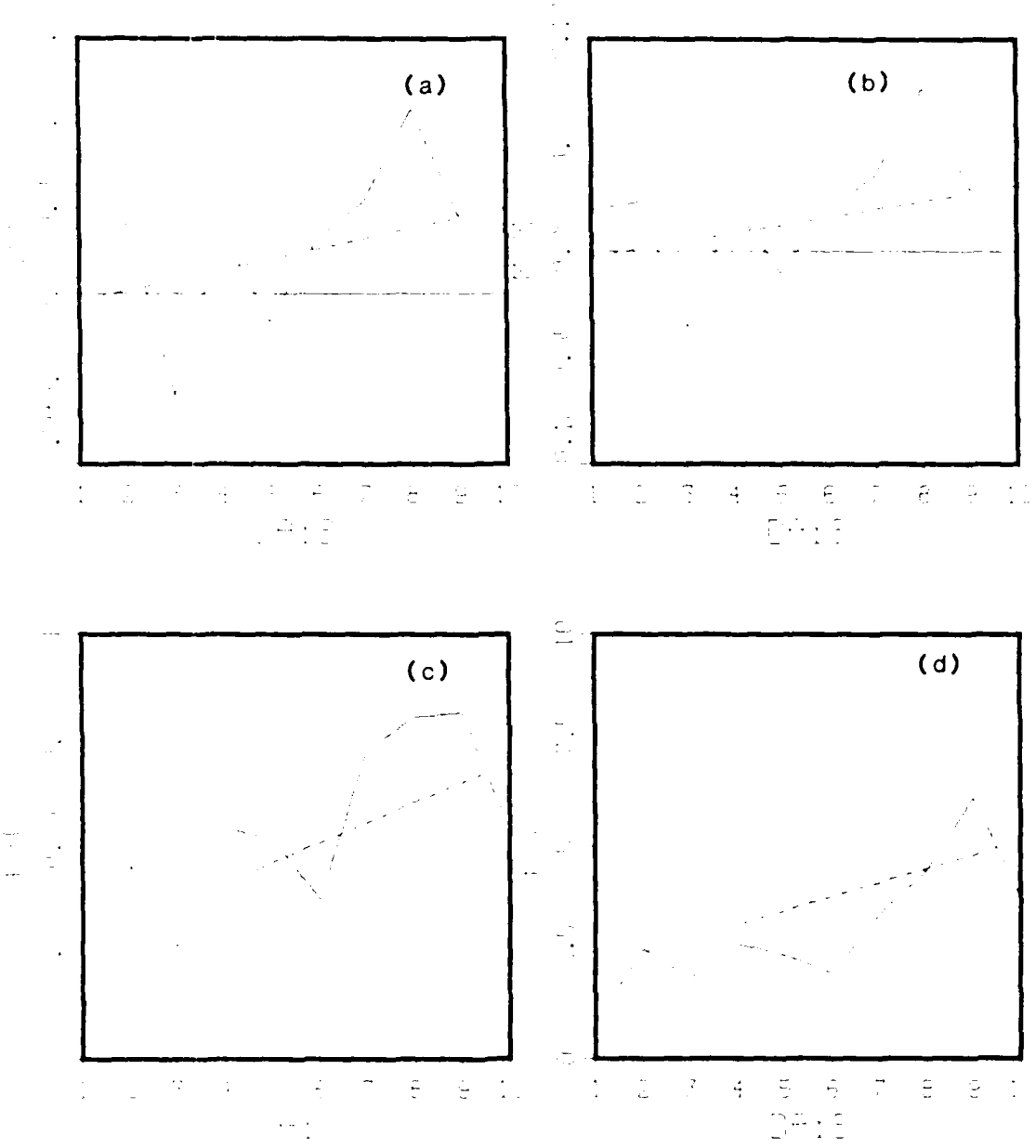

12. Similar to Fig. 10, except during April.

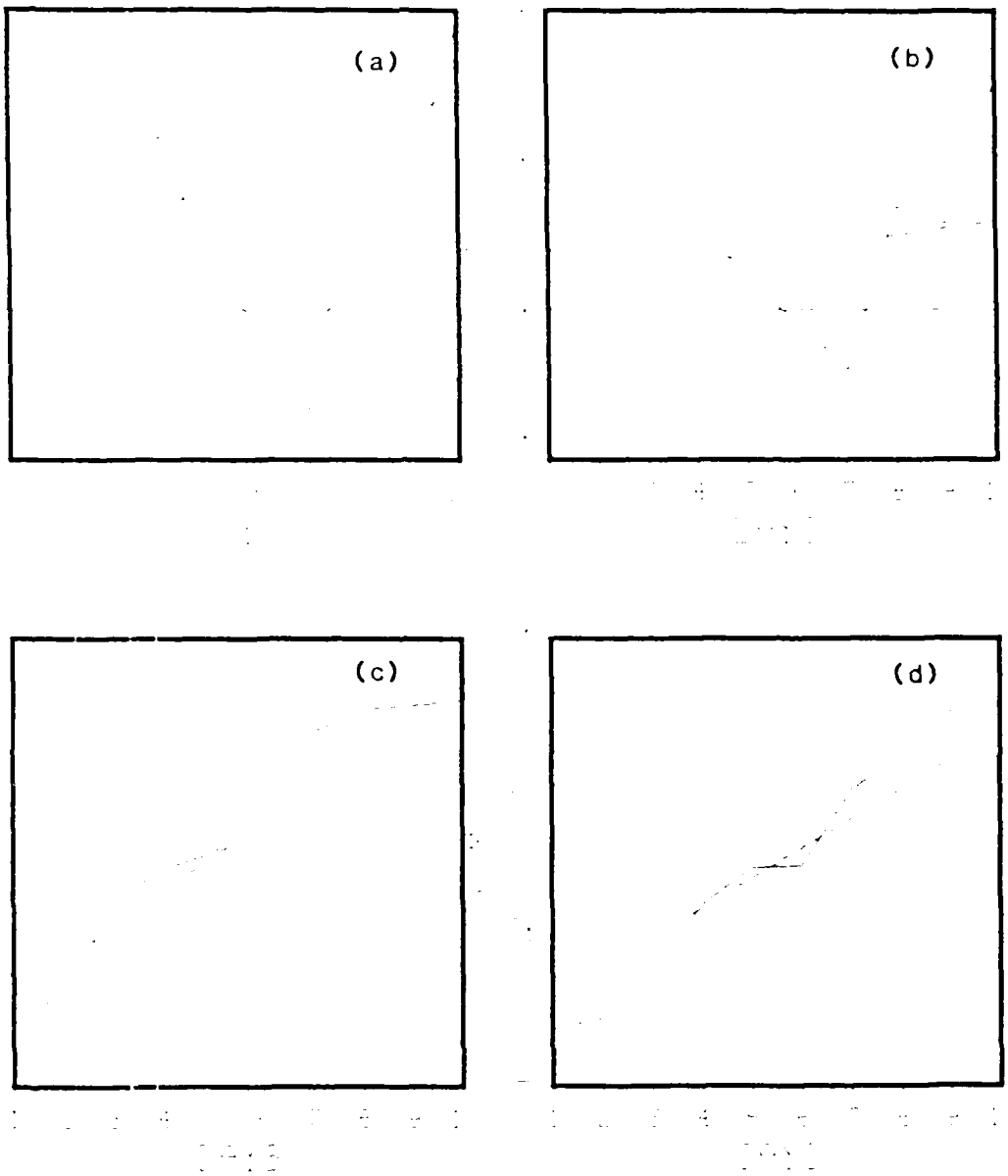

13. Similar to Fig. 12, except in Pacific region.

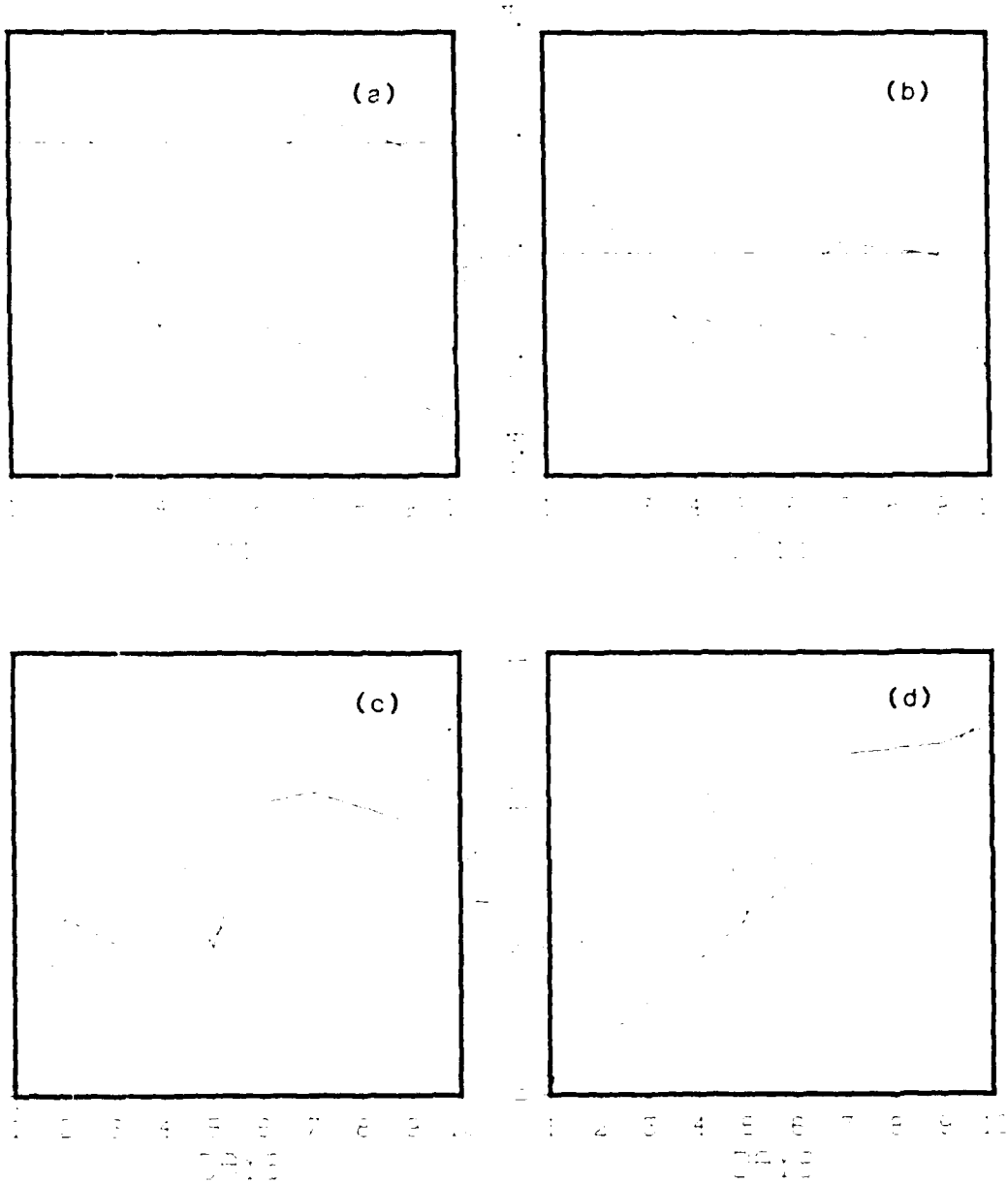

14. Field statistics for total heat flux during November in the Atlantic region. (a) Field-mean difference in gm-cal/cm²-h. (b) Ratio of field-mean difference to field-mean control. (c) Ratio of peak difference to peak control. (d) Ratio of peak difference to mean control.

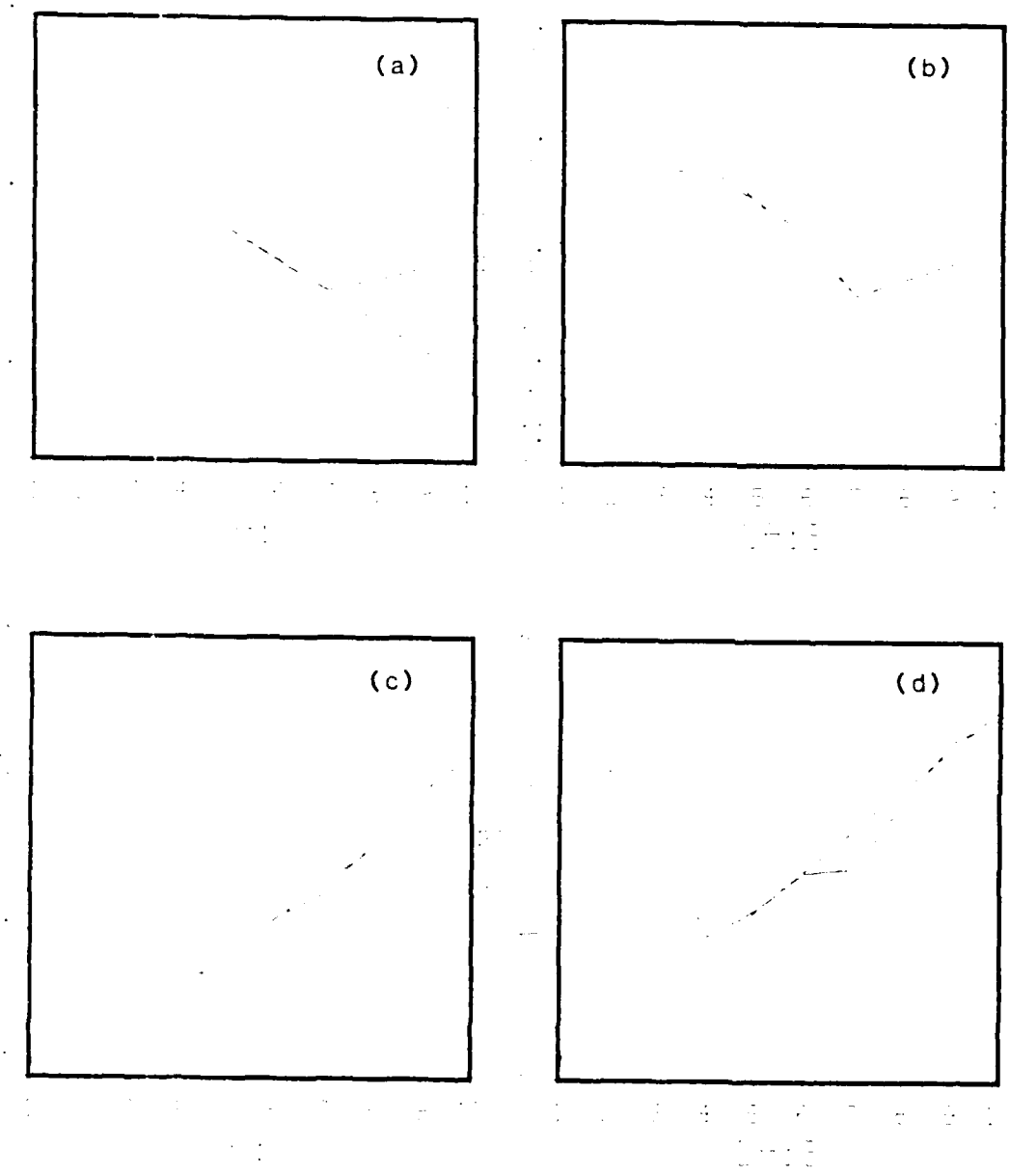

15. Similar to Fig. 14, except in Pacific region.

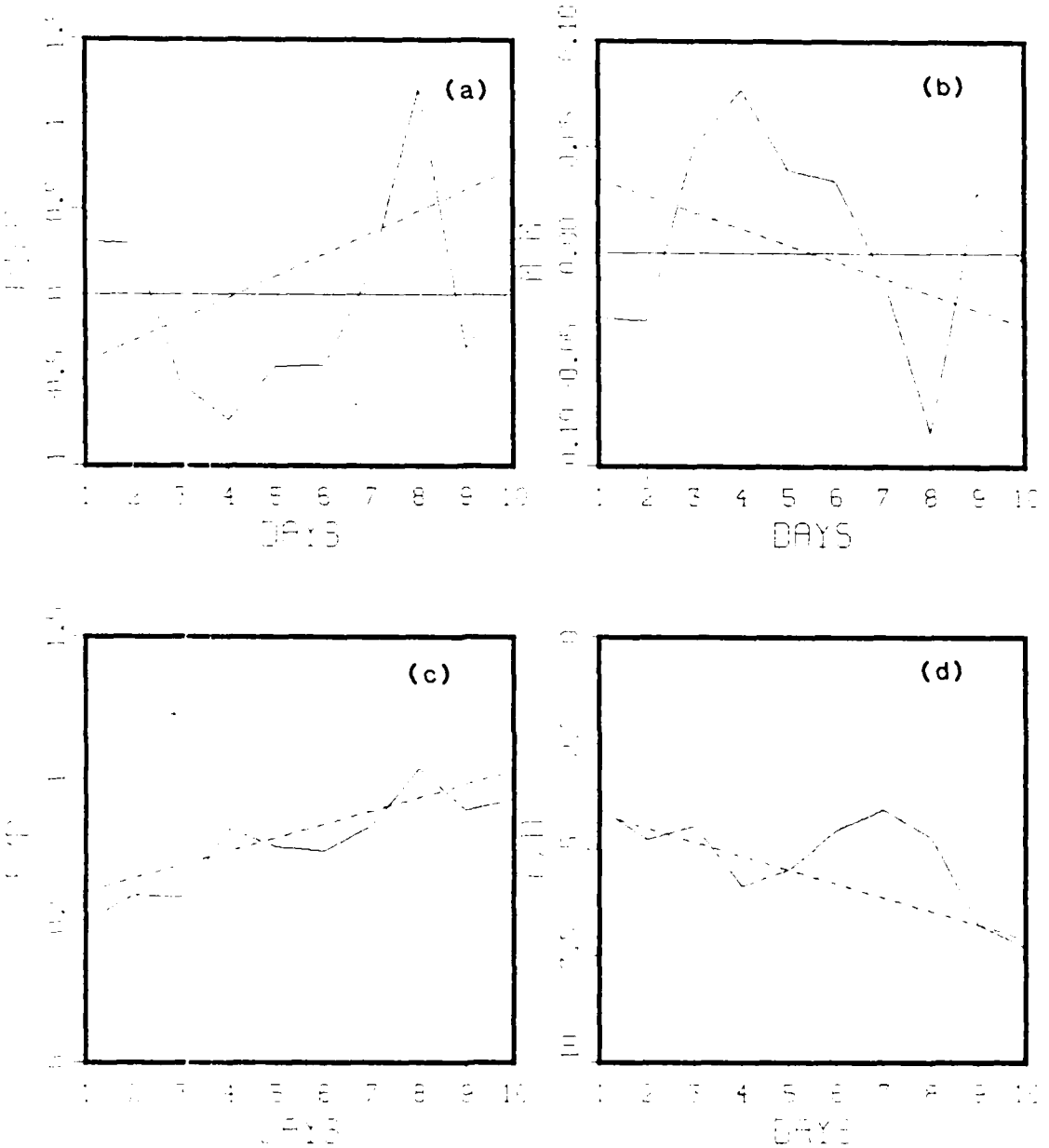

16. Similar to Fig. 14, except for April.

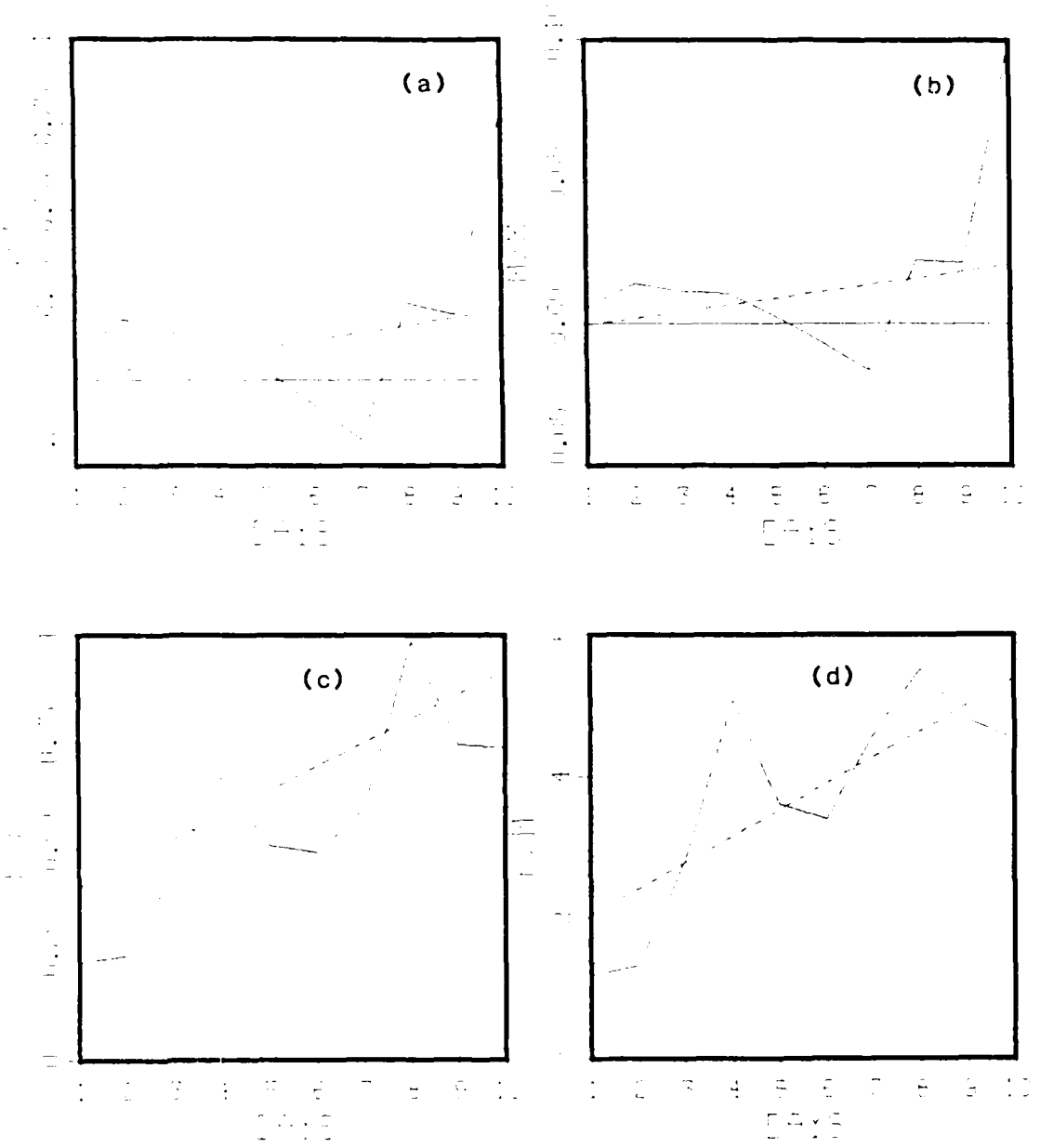

17. Similar to Fig. 16, except for Pacific region.

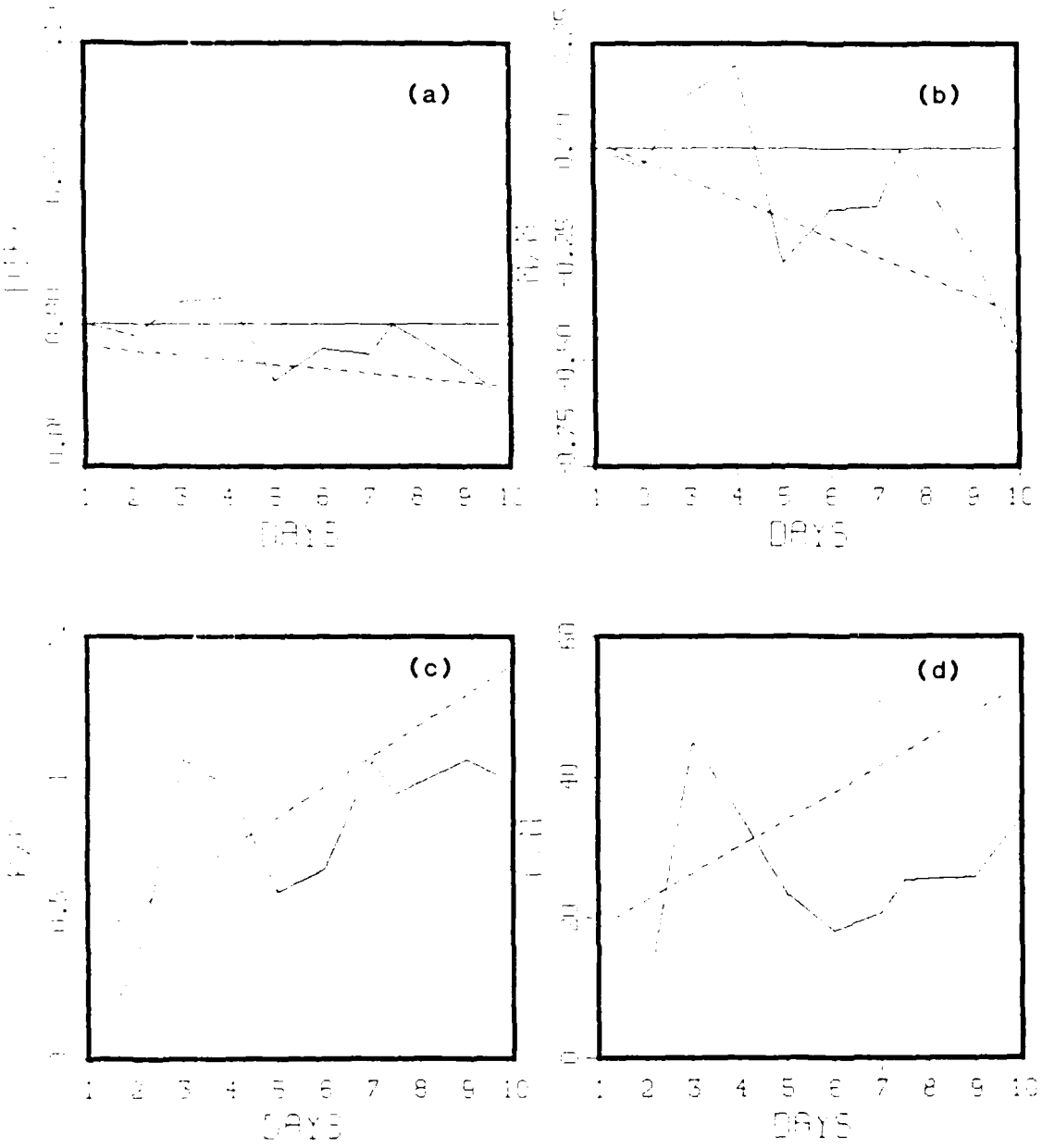

18. Field statistics for cumulus precipitation during November in the Atlantic region. (a) Field-mean difference in cm/day. (b) Ratio of field-mean difference to field-mean control. (c) Ratio of peak difference to peak control. (d) Ratio of peak difference to mean control.

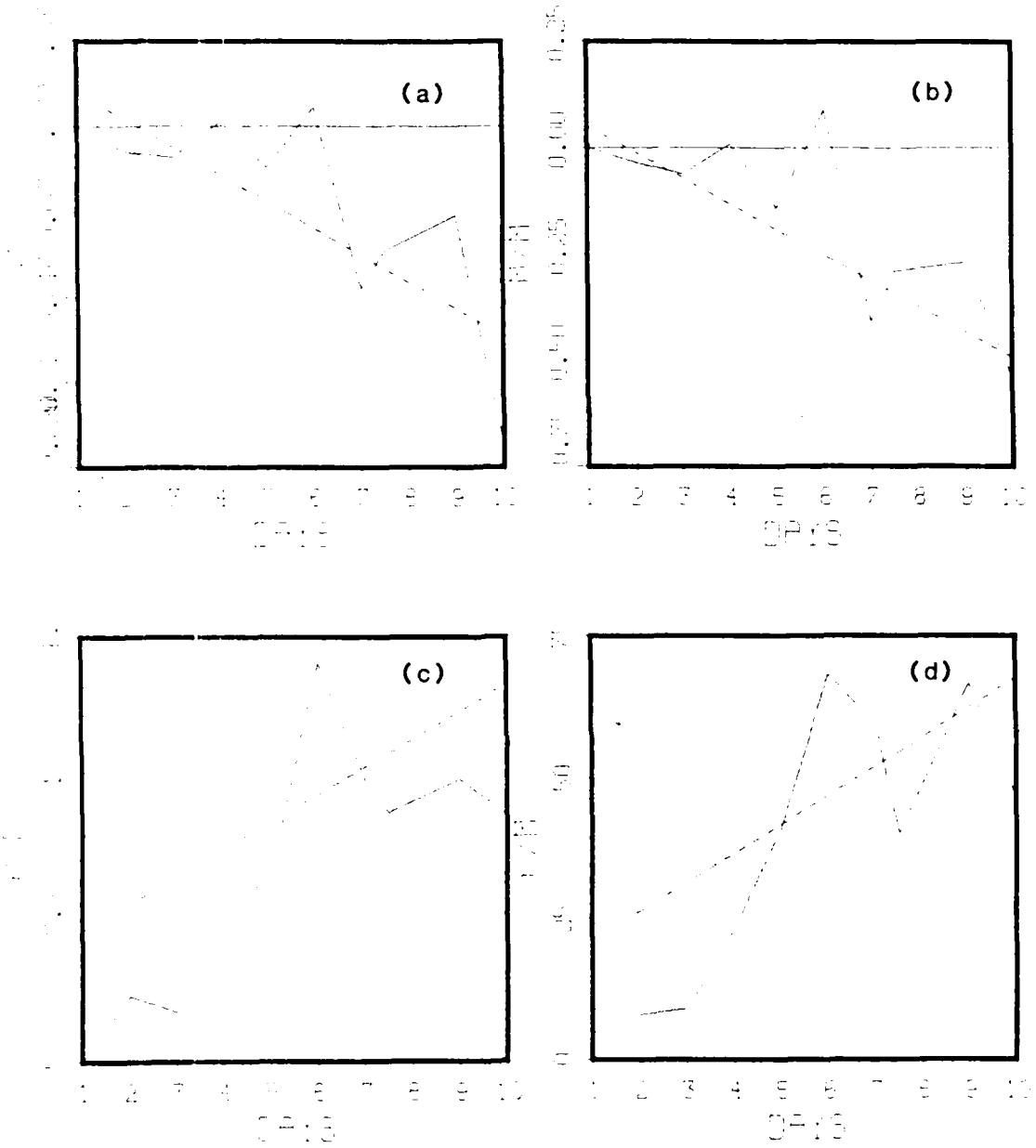

19. Similar to Fig. 18, except in the Pacific region.

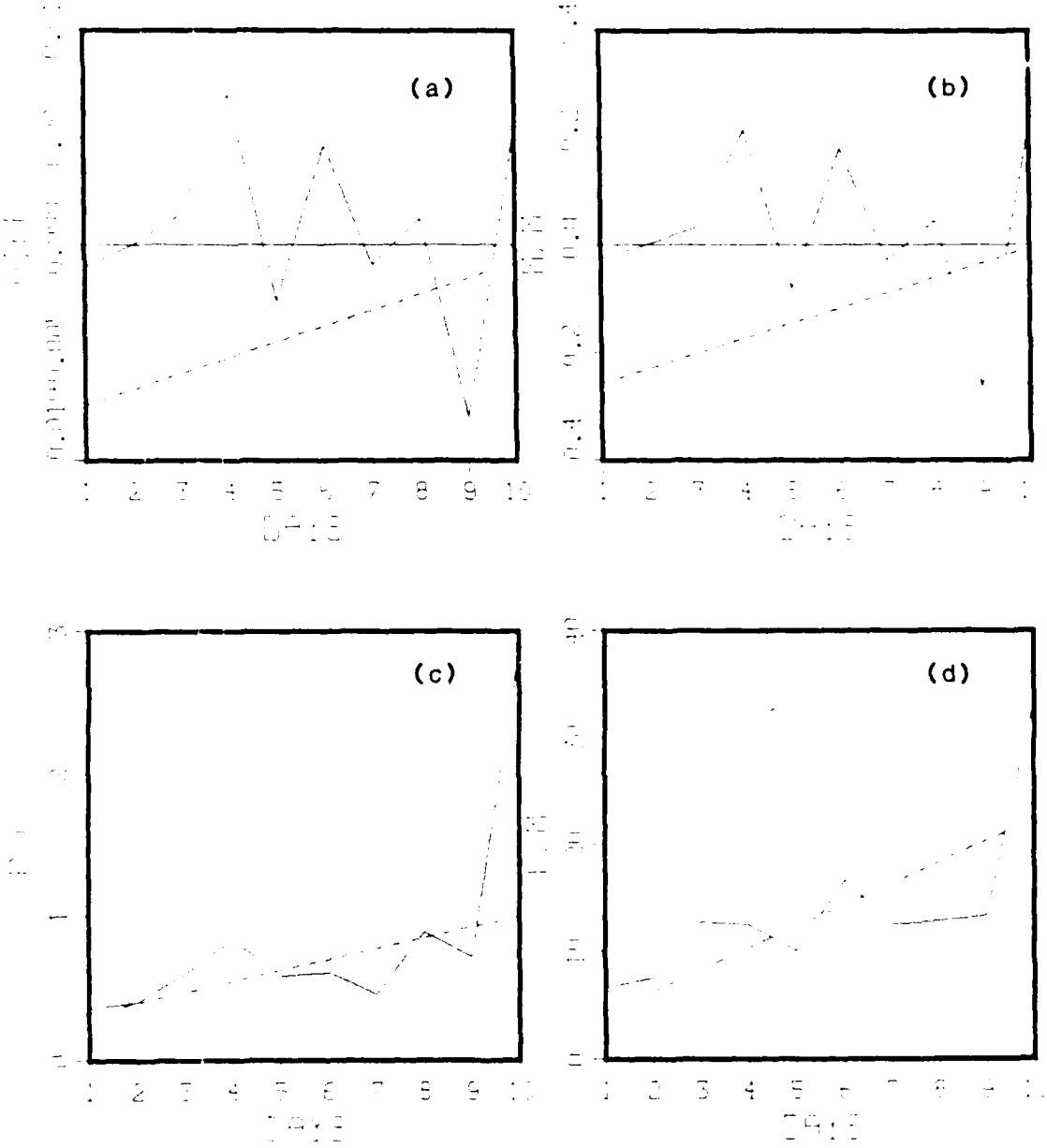

20. Similar to Fig. 18, except during April.

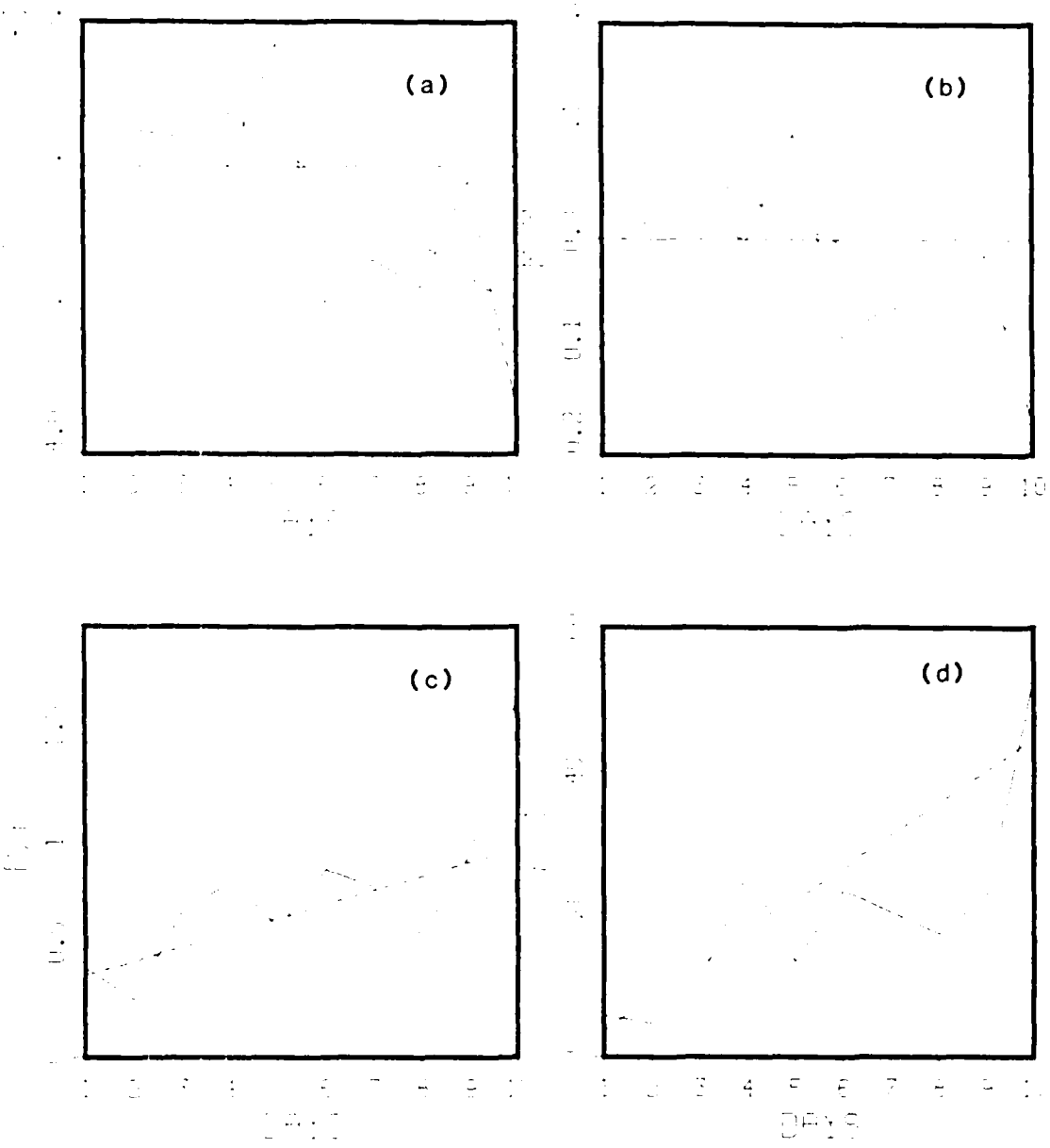

21. Similar to Fig. 20, except in the Pacific region.

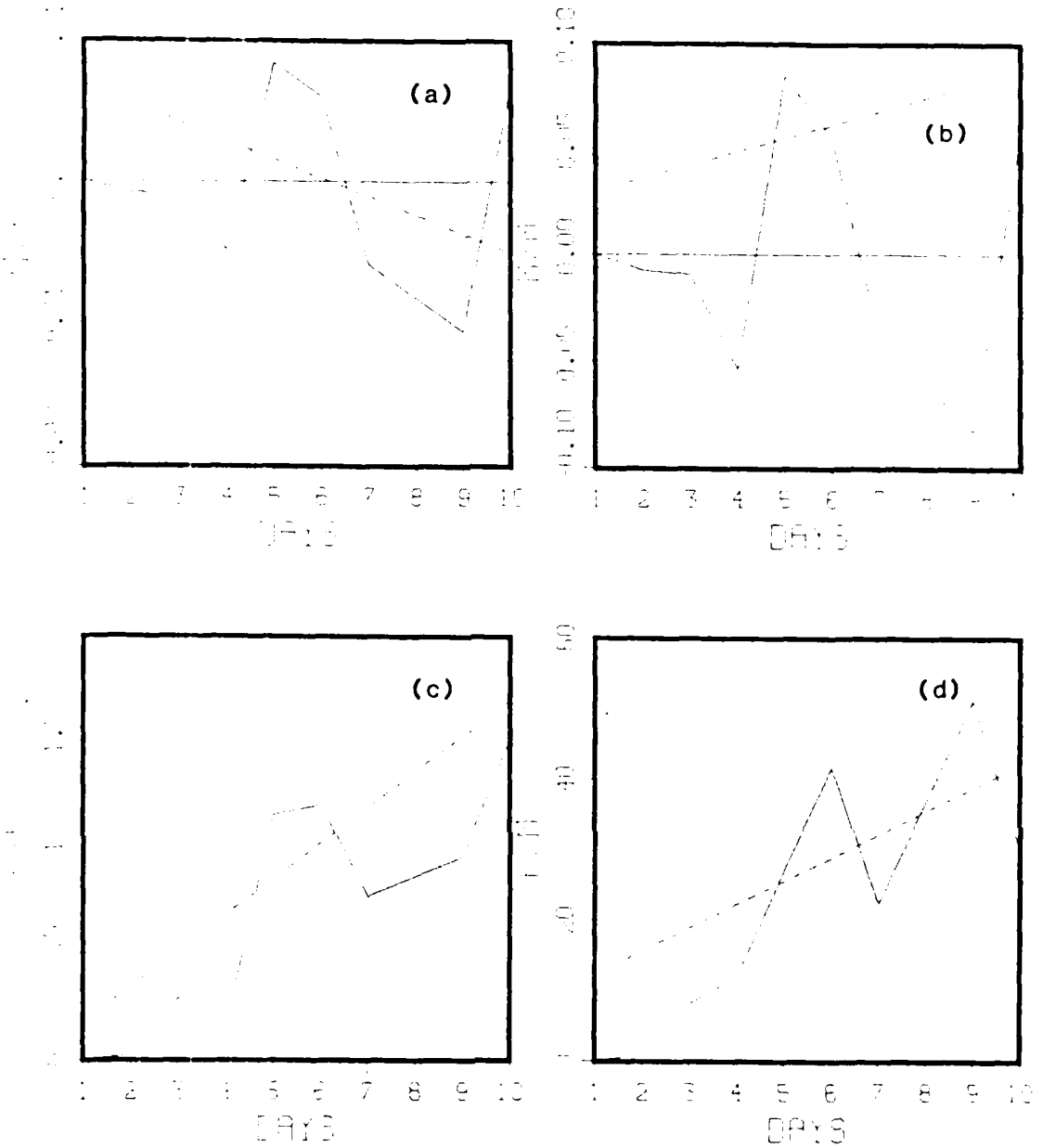

22. Field statistics for large-scale precipitation during November in the Atlantic region. (a) Field-mean difference in cm/day. (b) Ratio of field-mean difference to field-mean control. (c) Ratio of peak difference to peak control. (d) Ratio of peak difference to mean control.

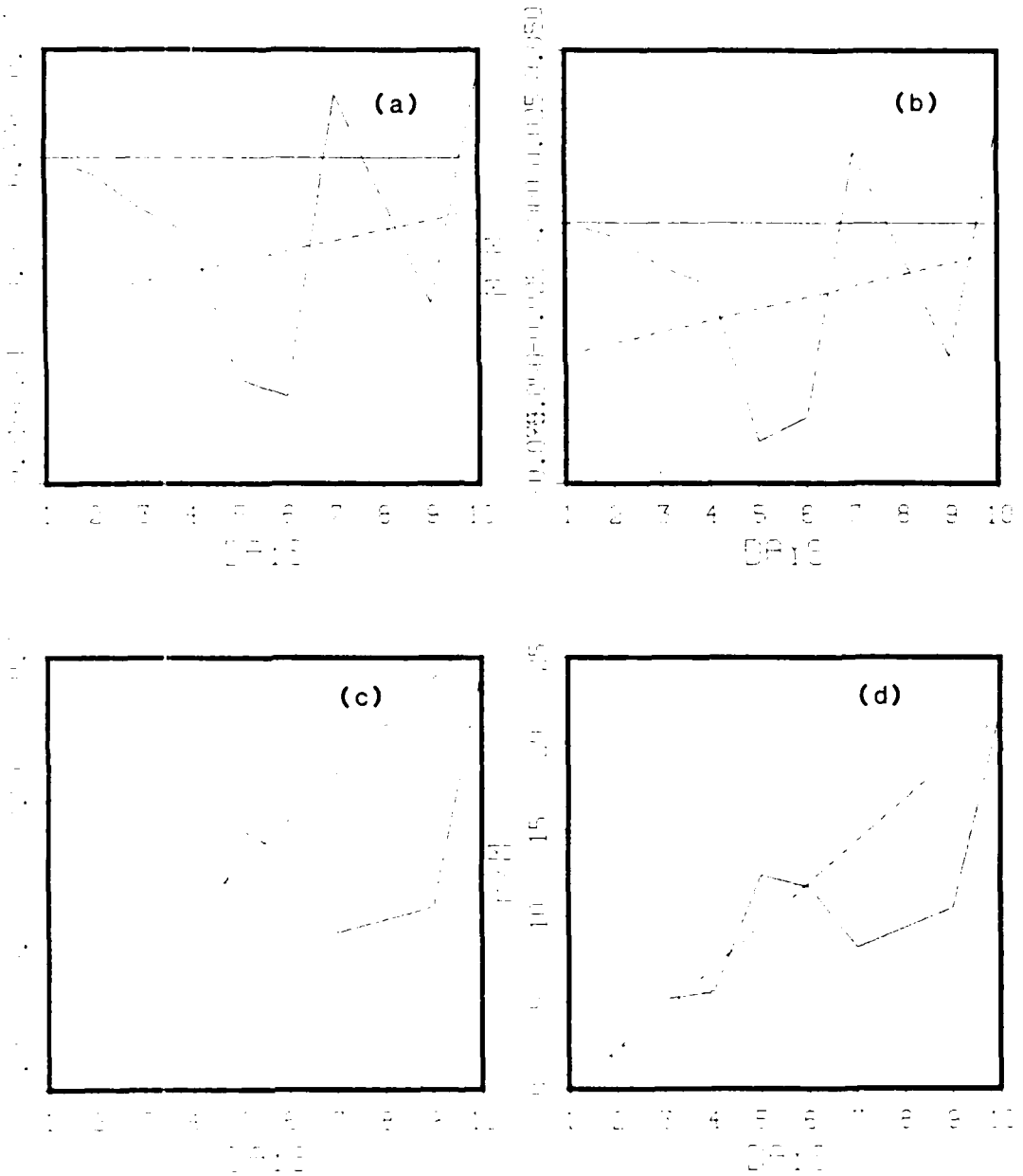

23. Similar to Fig. 22, except in the Pacific region.

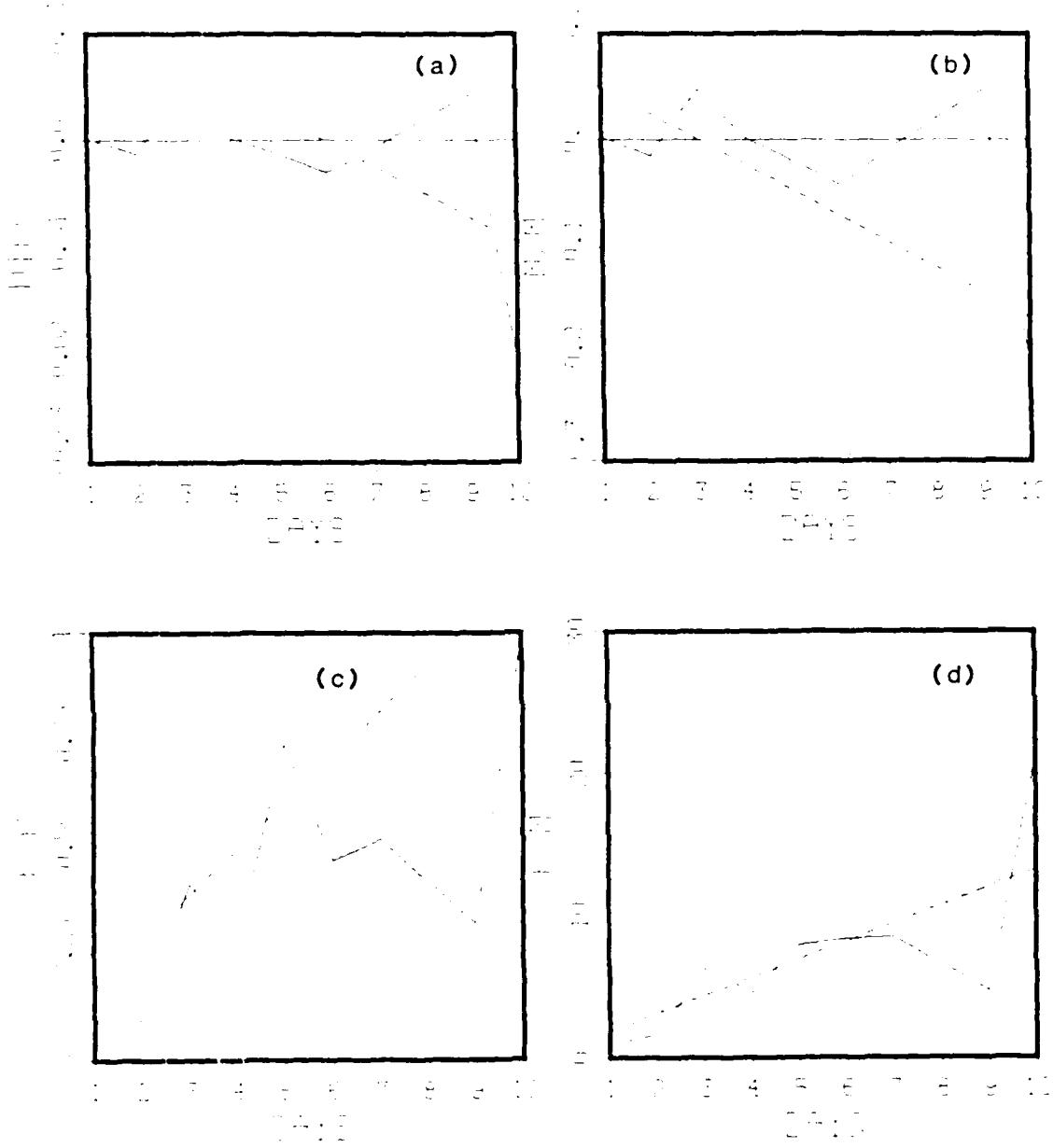

24. Similar to Fig. 22, except during April.

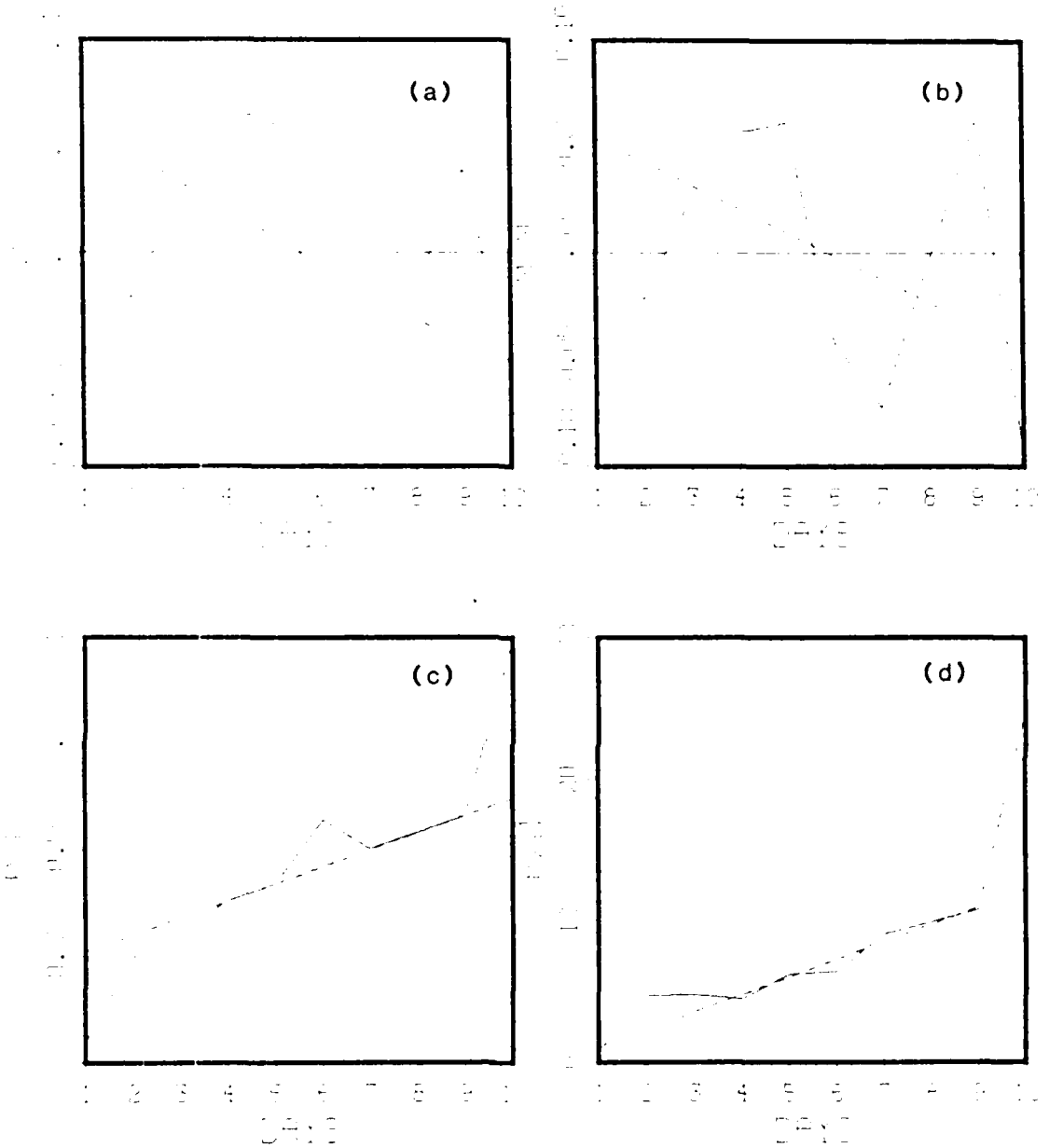

25. Similar to Fig. 24, except for the Pacific region.

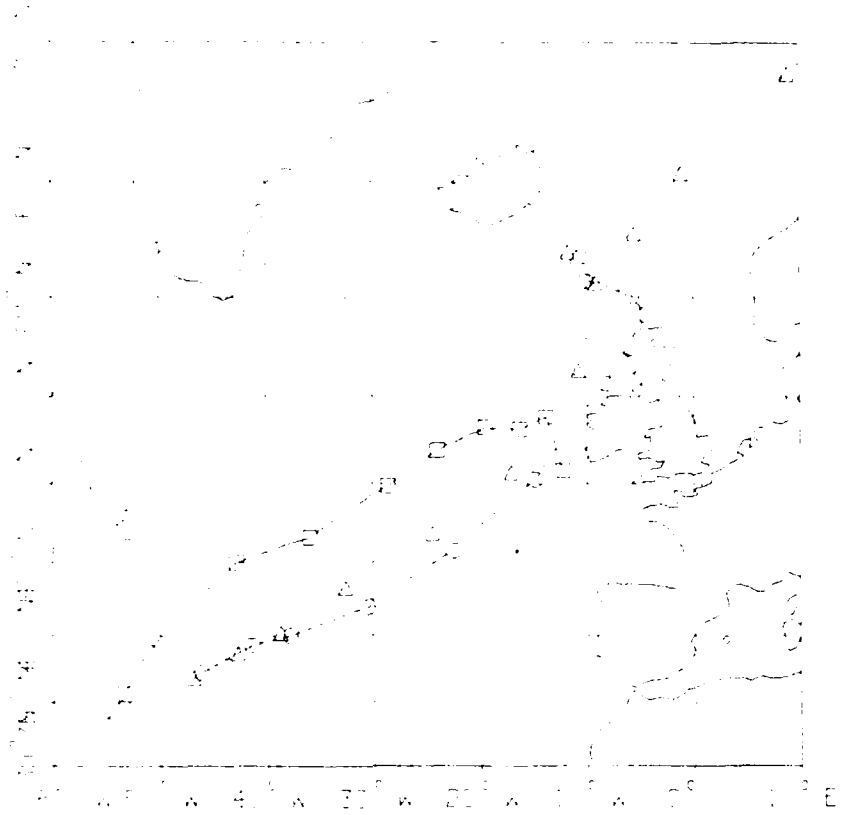

26. Storm tracks for storm NA5 which formed at tau= 72 hours. Symbols mark 12-hour analysis and forecast positions. Solid line is based on the analyses, dashed line is for control forecast and dotted line is for SST forecast.

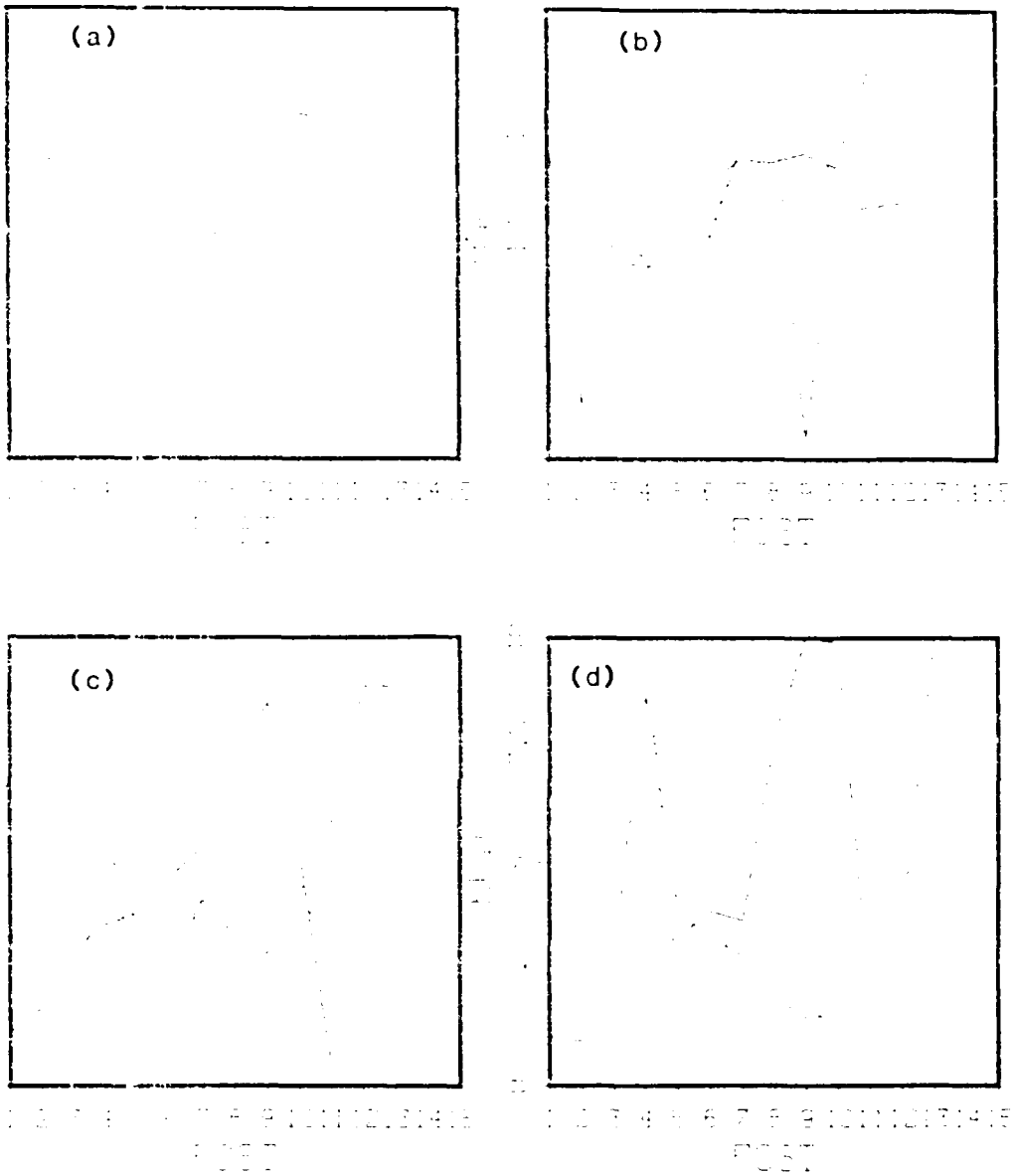

27. (a) Amplitude, (b) angle, (c) radius and (d) ellipticity for storm NA5 based on analyses (solid), control forecast (dashed) and SST forecast (dotted).

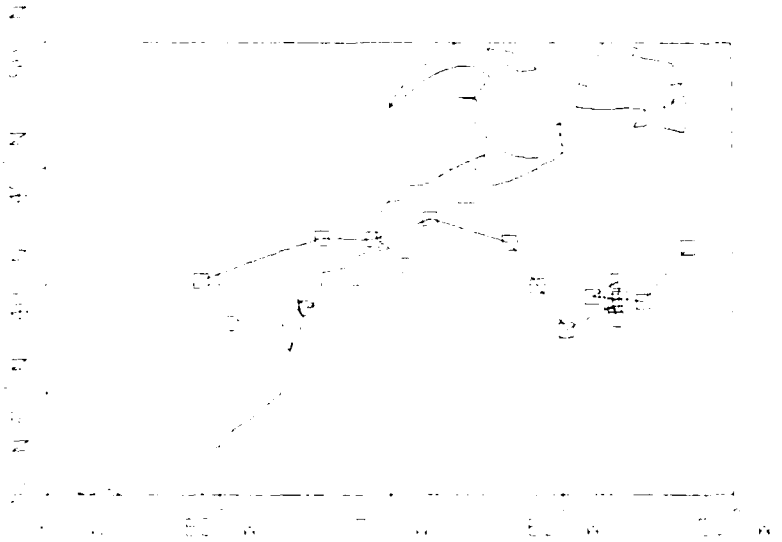

28. Similar to Fig. 26, except for storm AA3 which formed at tau= 84 hours.

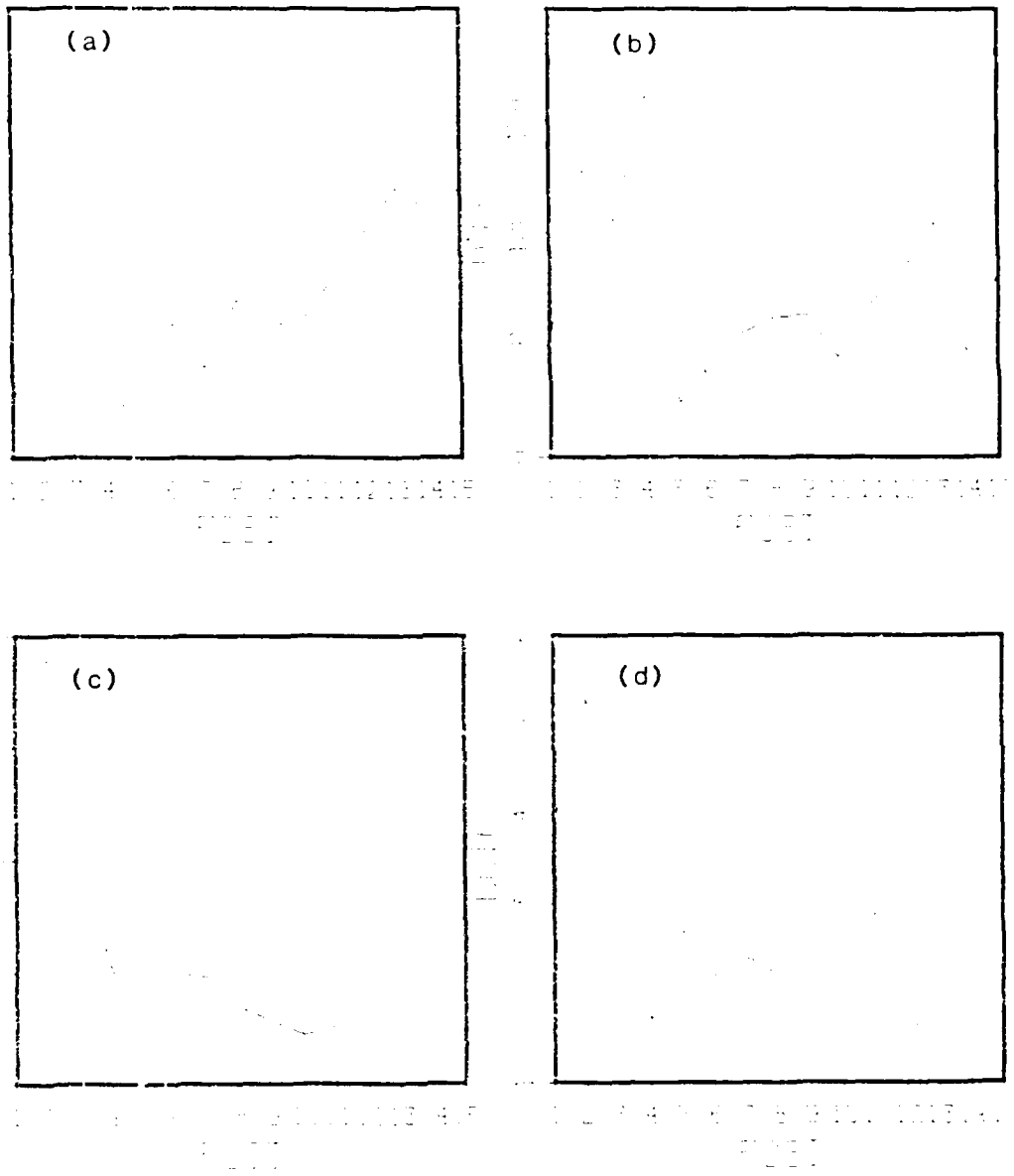

28. Similar to Fig. 27, except for storm AA3.

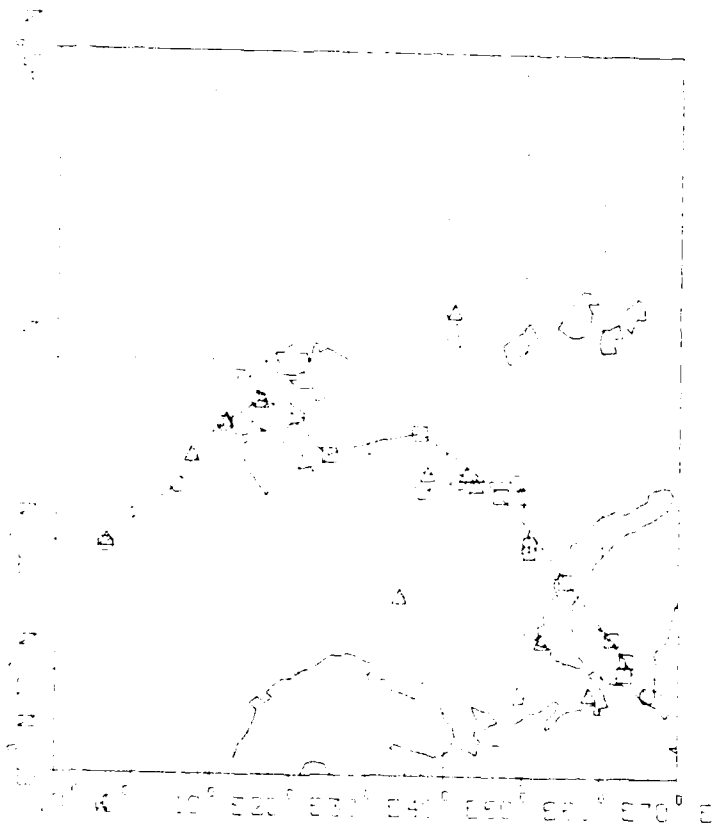

30. Similar to Fig. 26, except for storm AA4 which formed at tau= 120 hours.

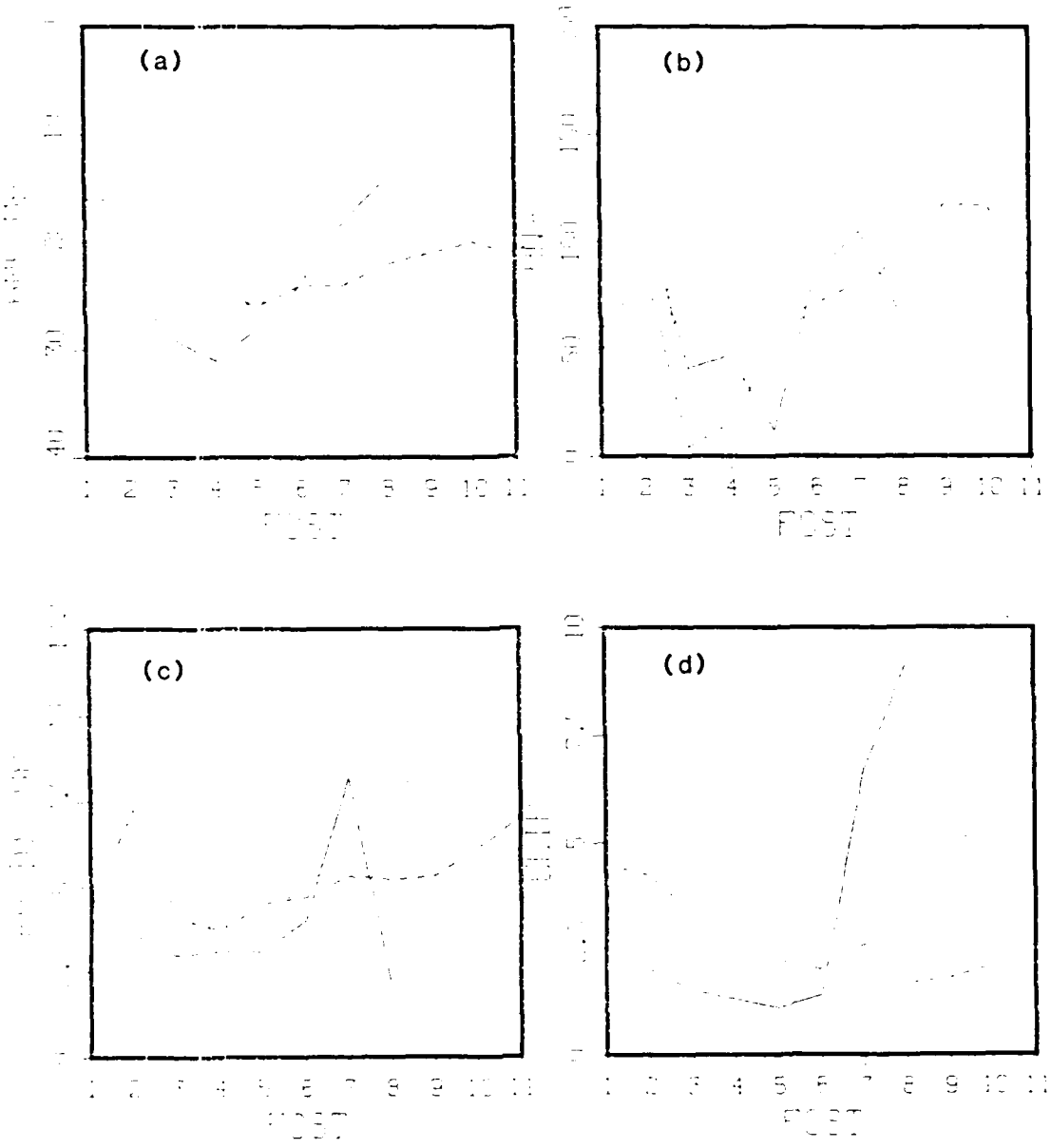

31. Similar to Fig. 27, except for storm AA4.

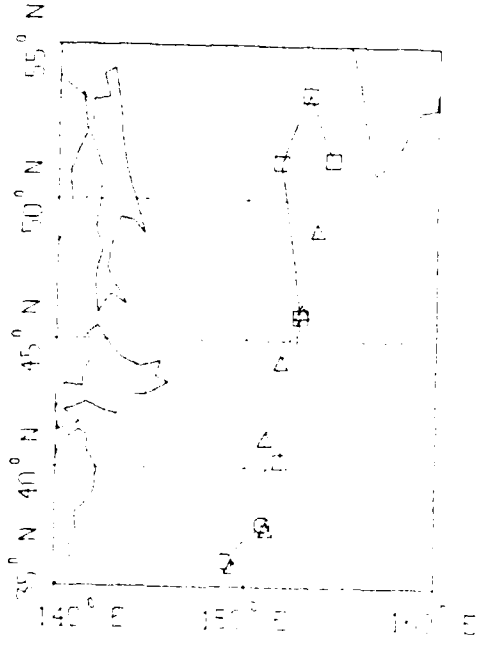

32. Similar to Fig. 26, except for storm AP3 which formed at tau= 60 hours.

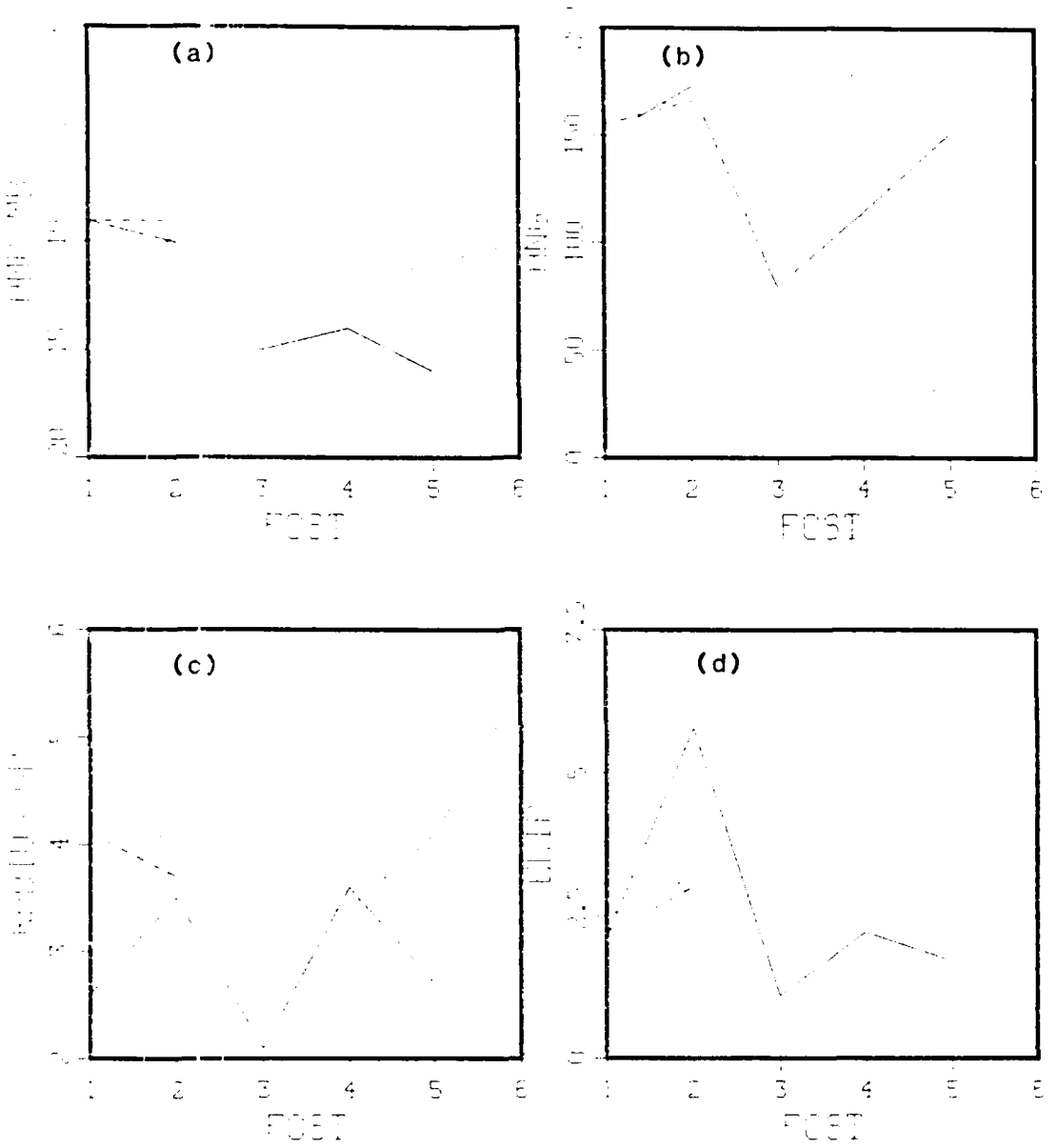

33. Similar to Fig. 27, except for storm AP3.

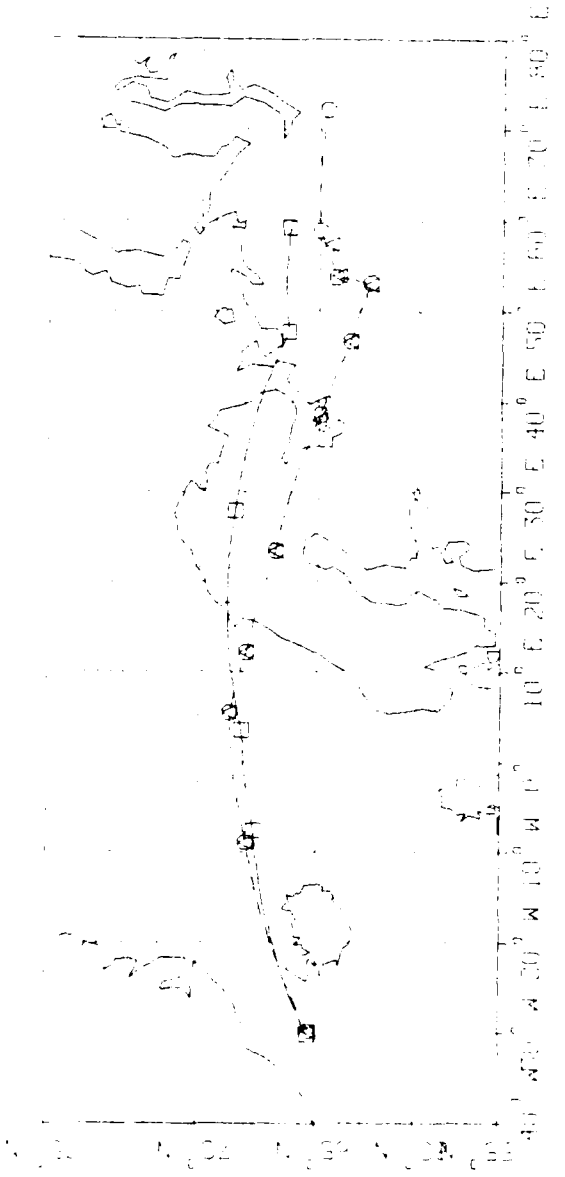

34. Similar to Fig. 26, except for storm NA1 which was present in the initial conditions.

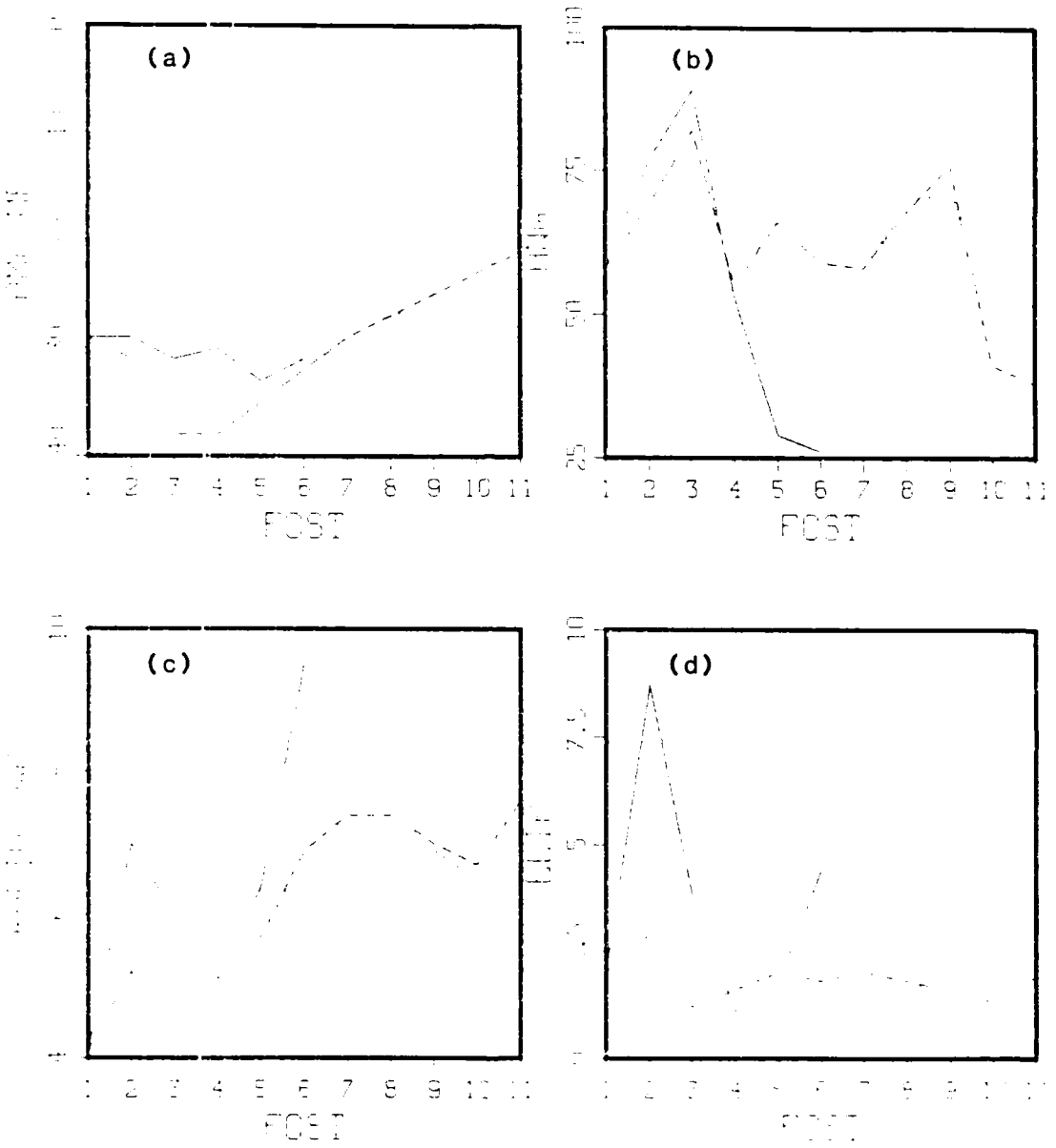

35. Similar to Fig. 27, except for storm NA1.

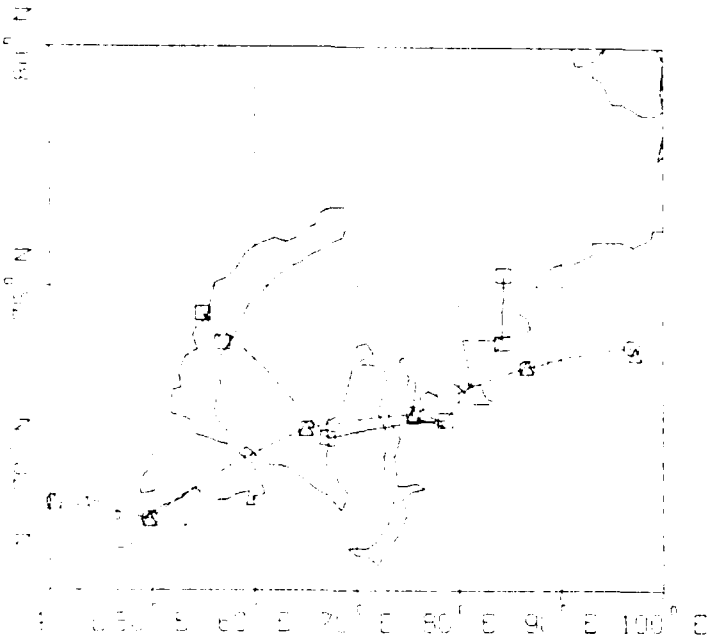

36. Similar to Fig. 26, except for storm NA2 which was present in the initial conditions.

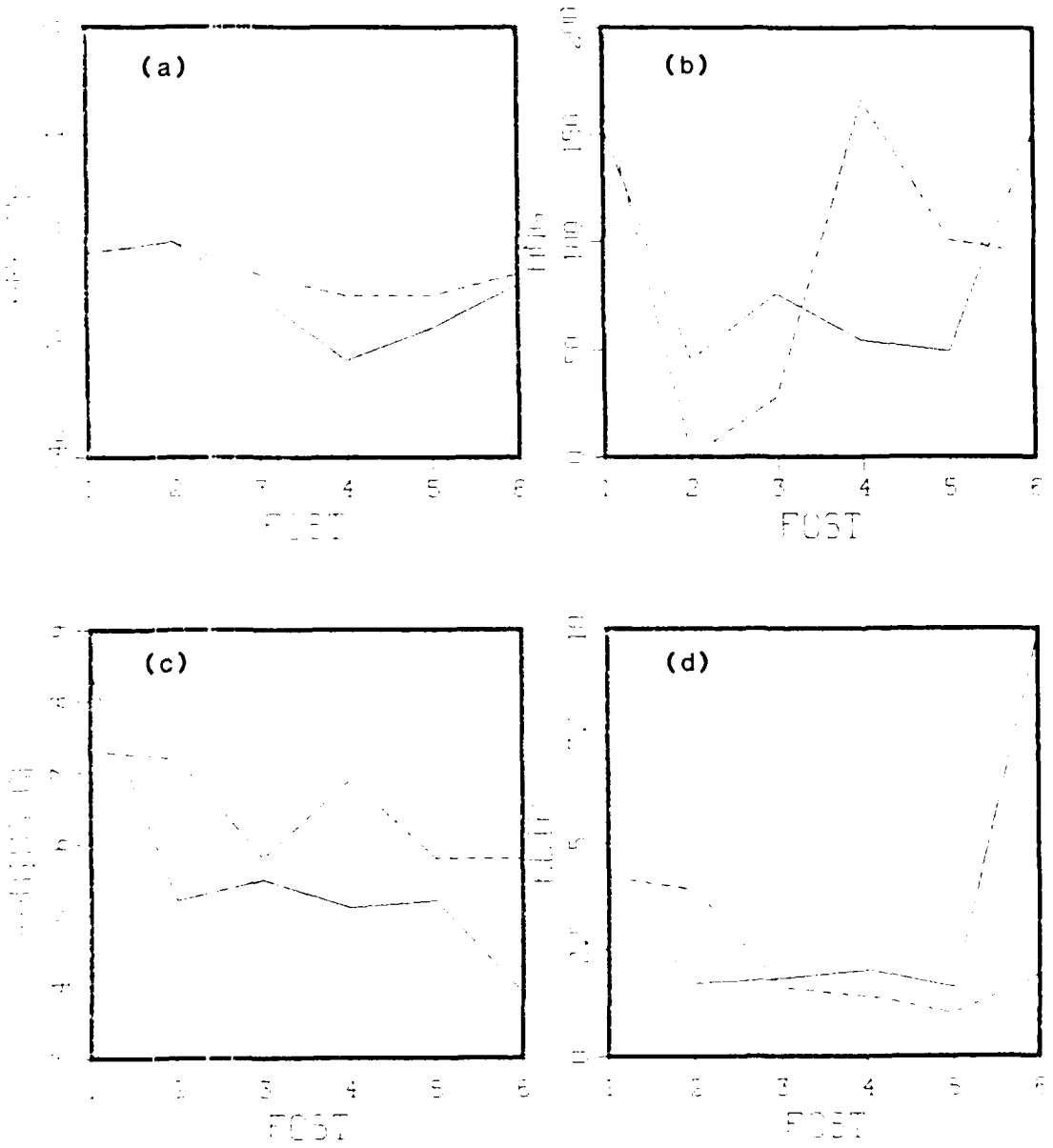

37. Similar to Fig. 27, except for storm NA2.

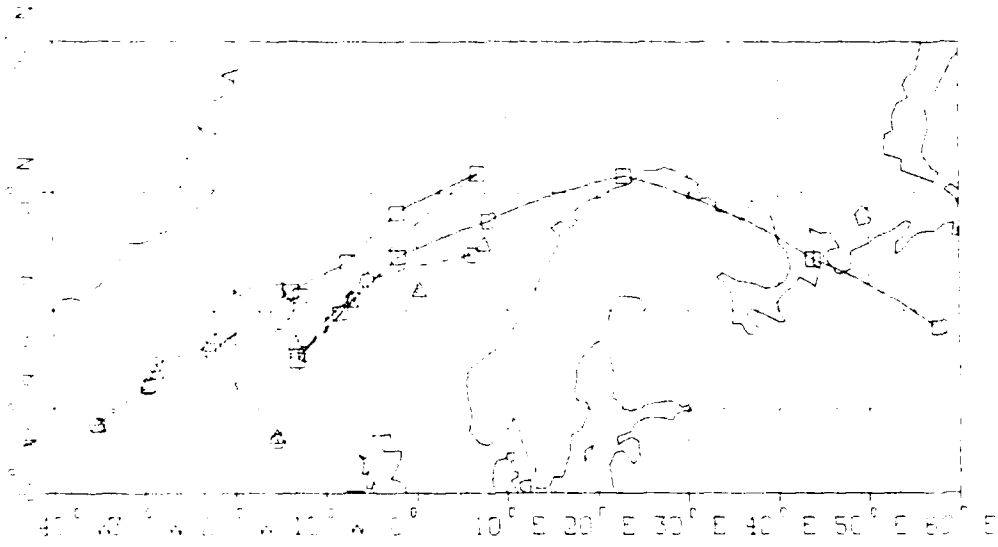

38. Similar to Fig. 26, except for storm NA3 which formed at tau= 72 hours.

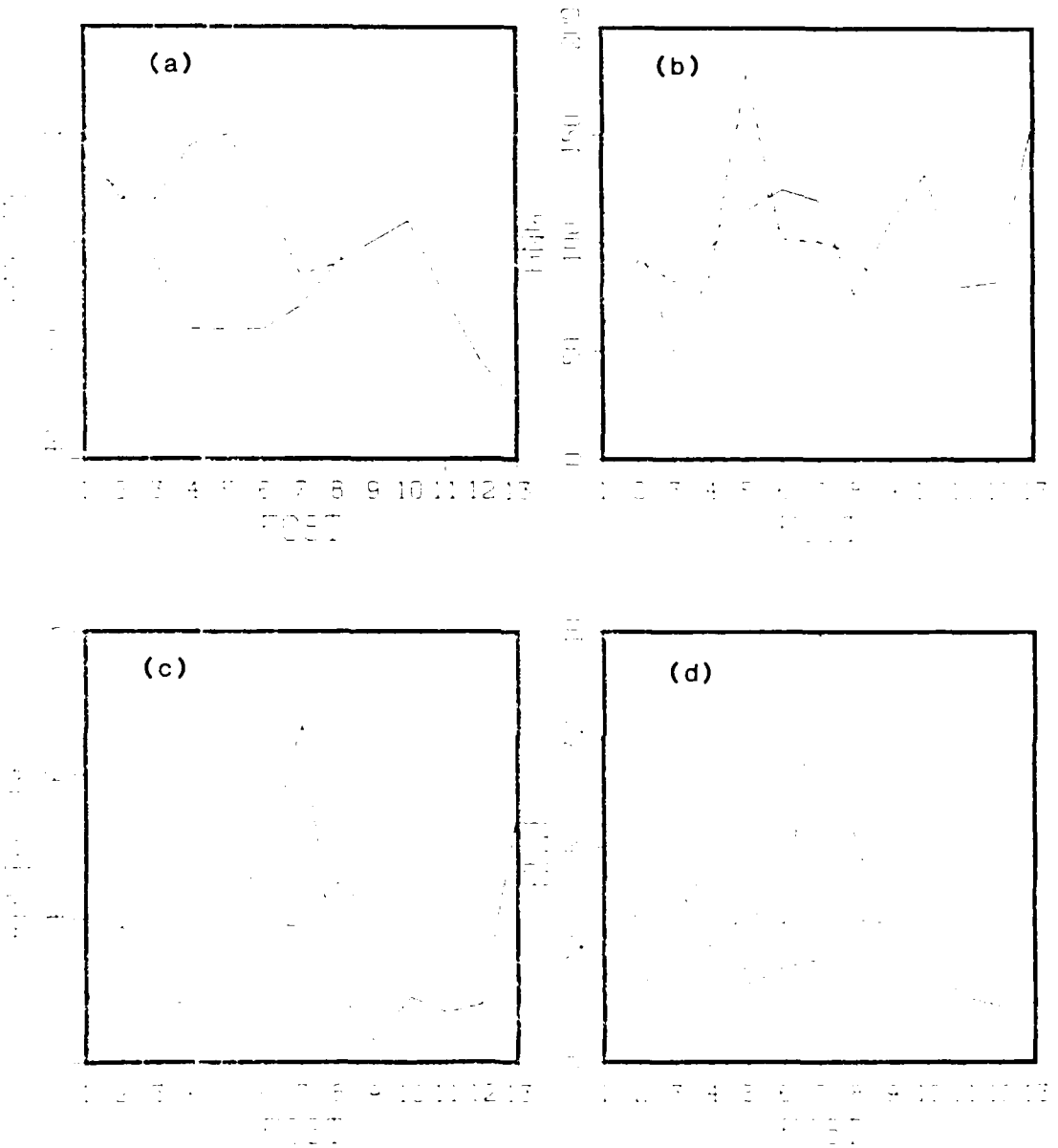

39. Similar to Fig. 27, except for storm NA3.

40. Similar to Fig. 26, except for storm NA4 which formed at tau= 72 hours.

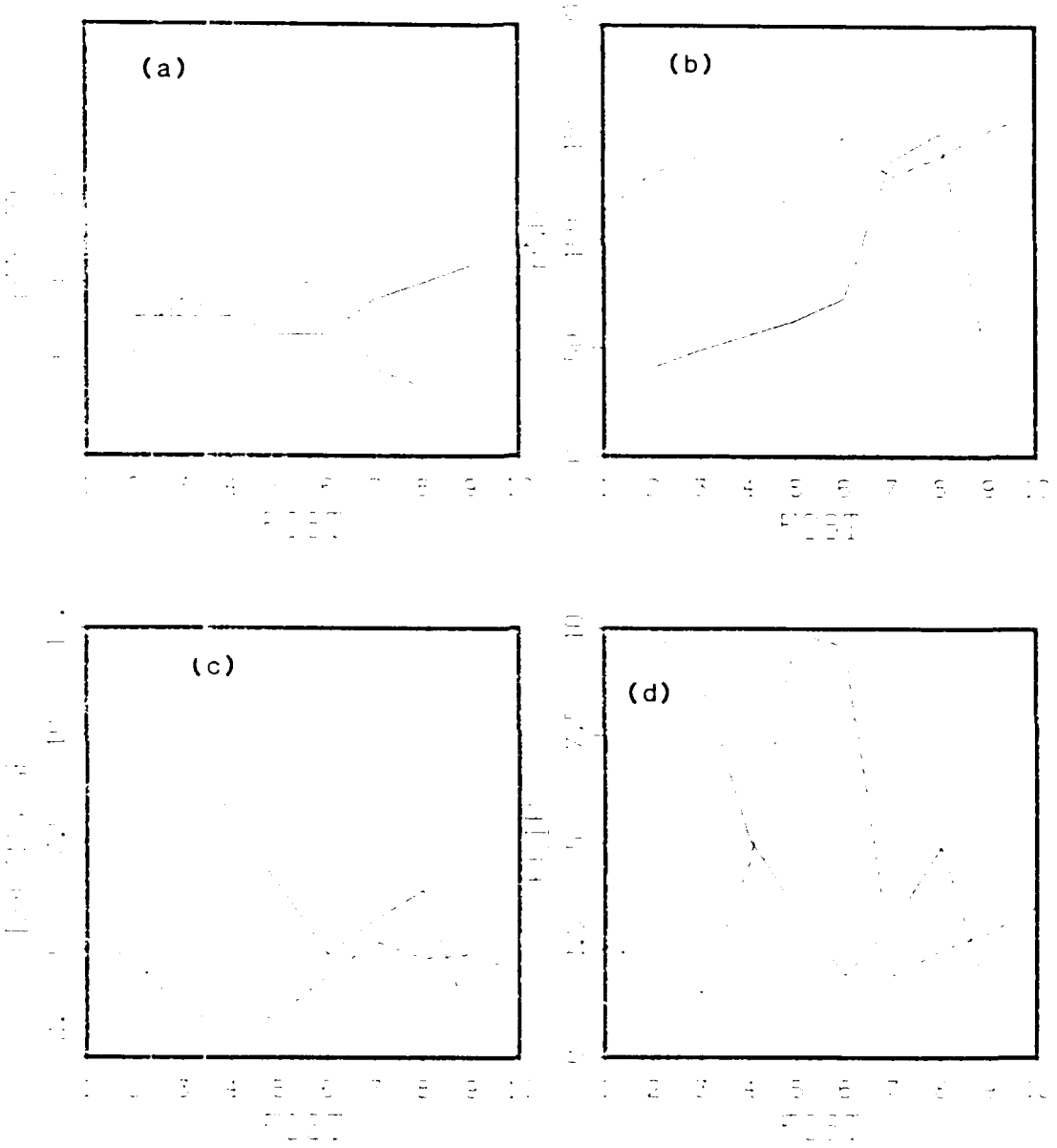

41. Similar to Fig. 27, except for storm NA4.

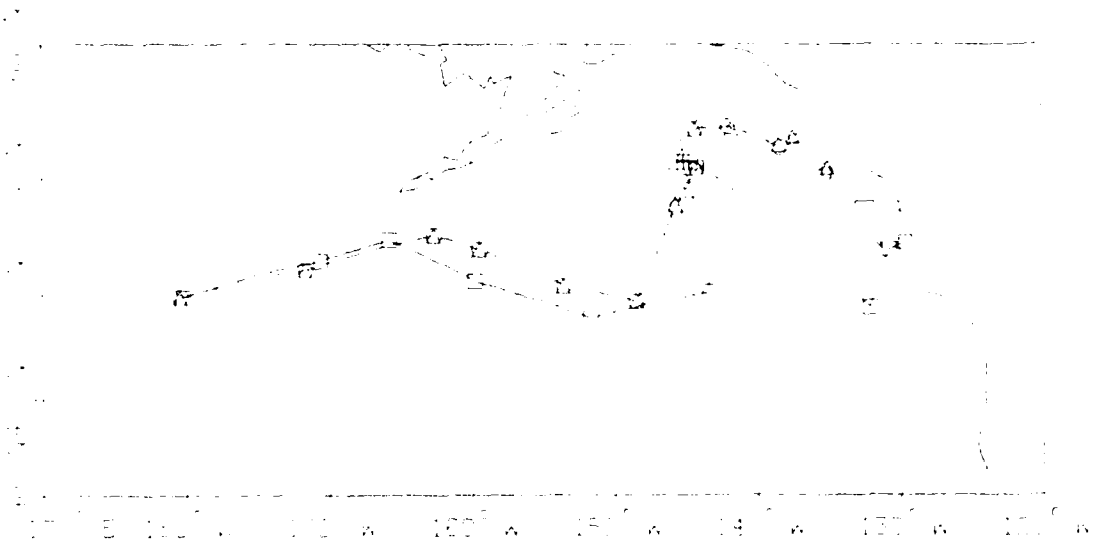

42. Similar to Fig. 26, except for storm NP1 which was present in the initial conditions.

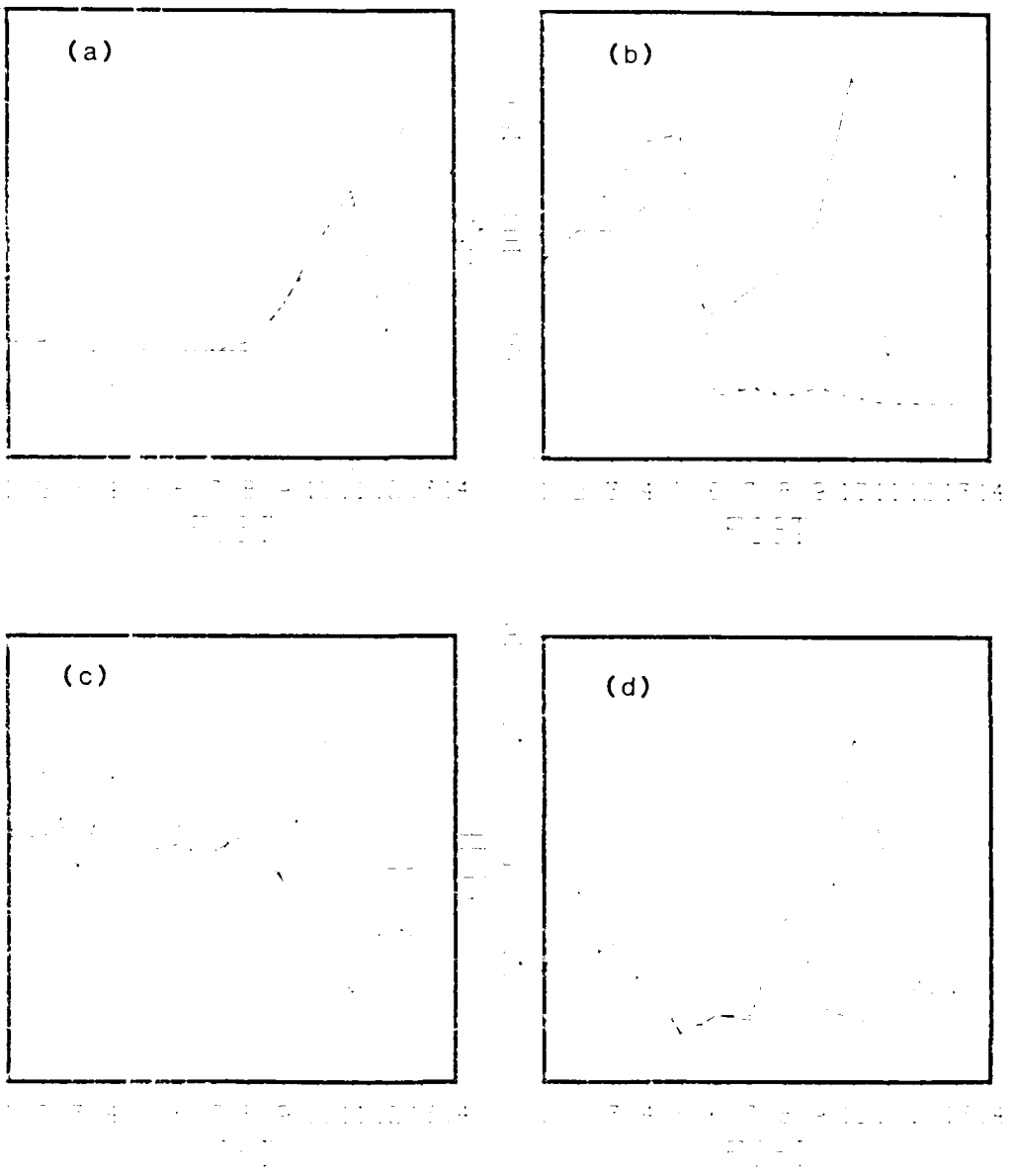

47. Similar to Fig. 27, except for storm NP1.

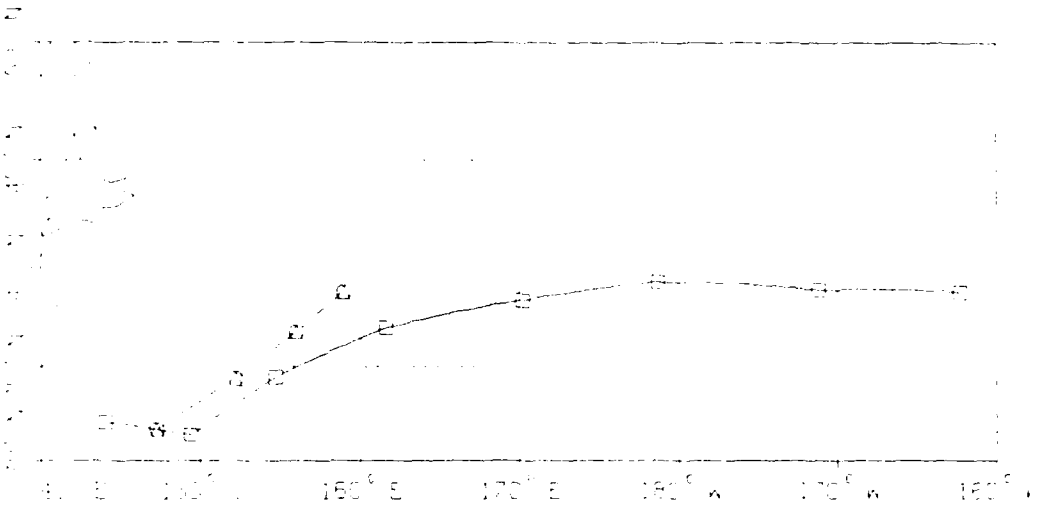

44. Similar to Fig. 26, except for storm NP2 which formed at tau= 24 hours.

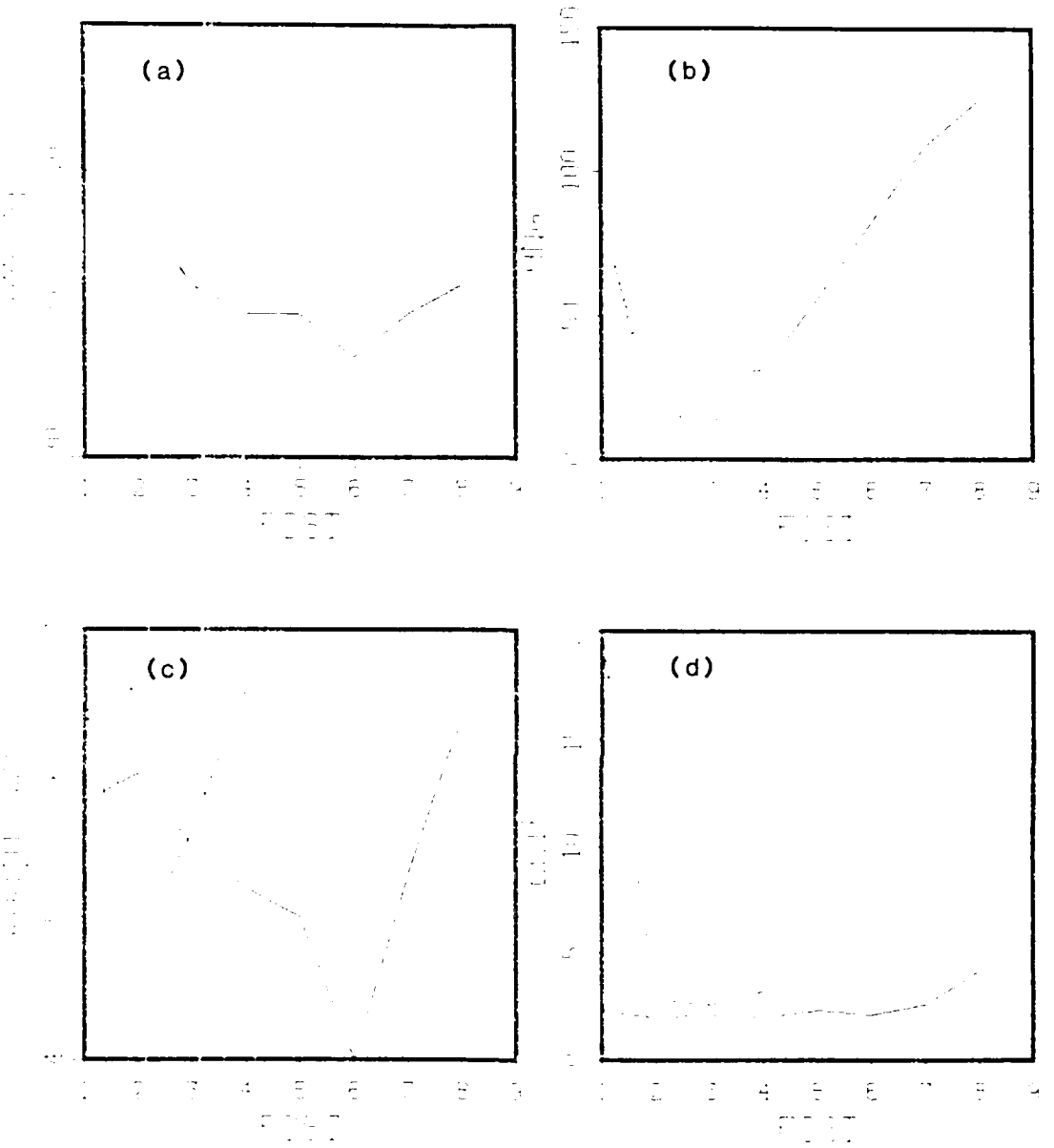

45. Similar to Fig. 27, except for storm NP2.

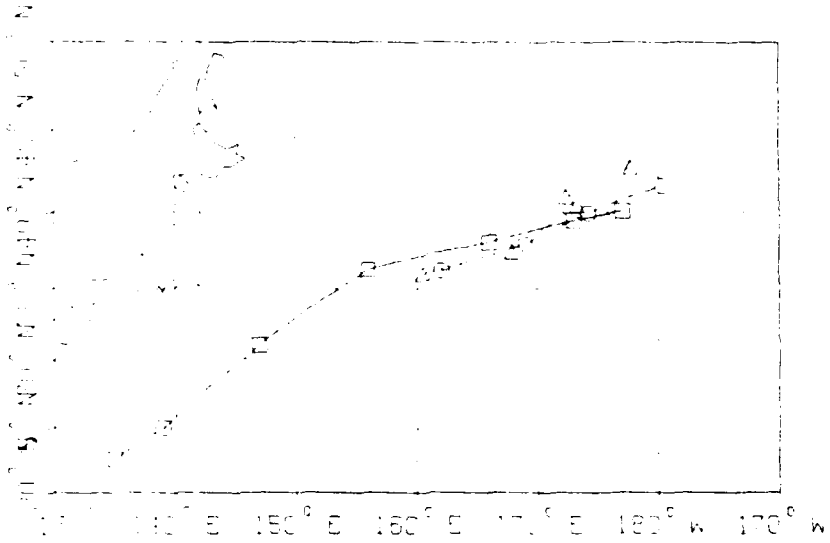

46. Similar to Fig. 26, except for storm NP3 which formed at tau= 120 hours

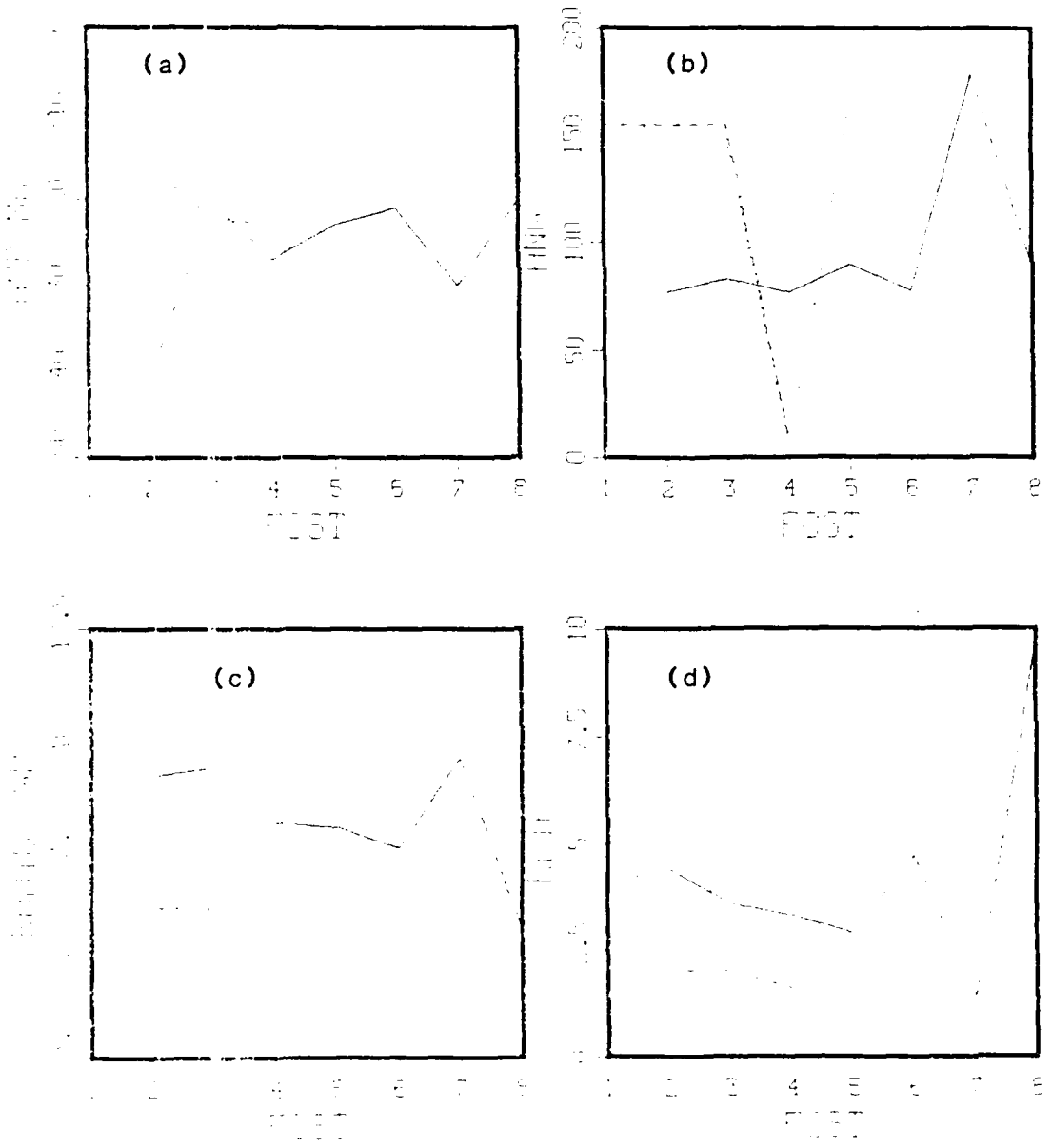

47. Similar to Fig. 27, except for storm NP3.

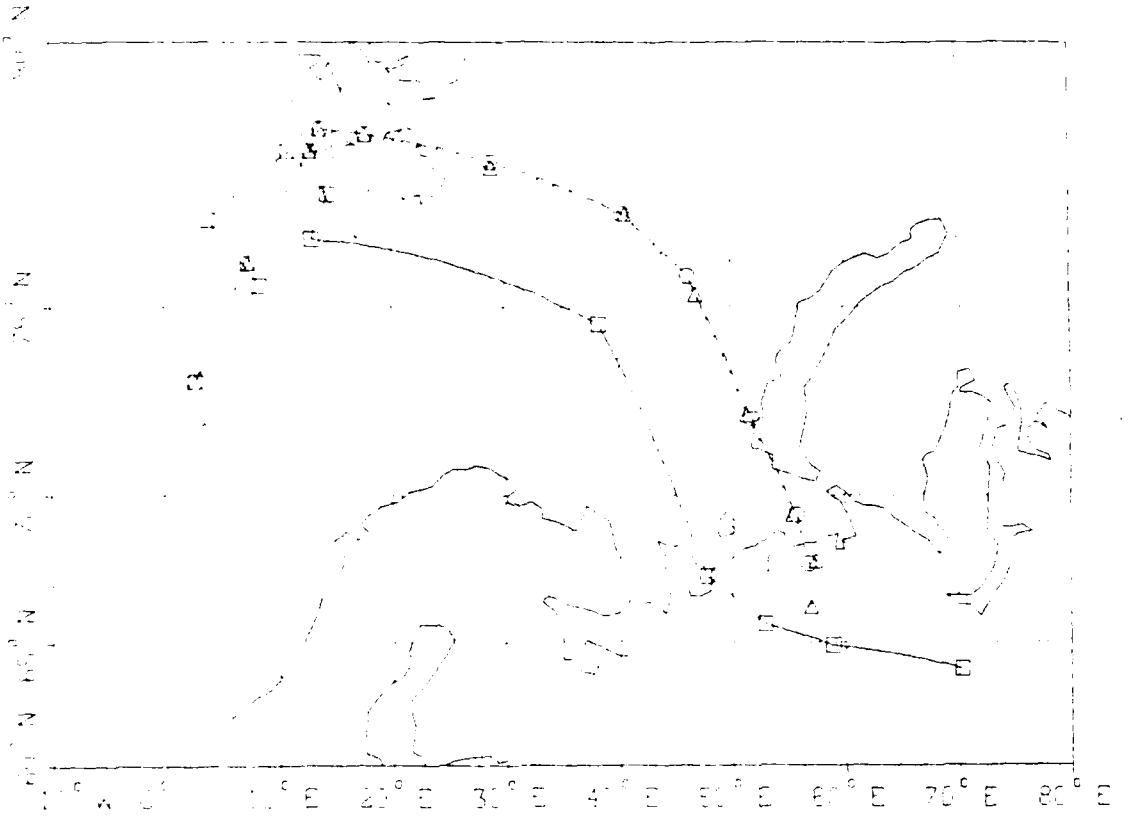

48. Similar to Fig. 26, except for storm AA1 which was present in the initial conditions.

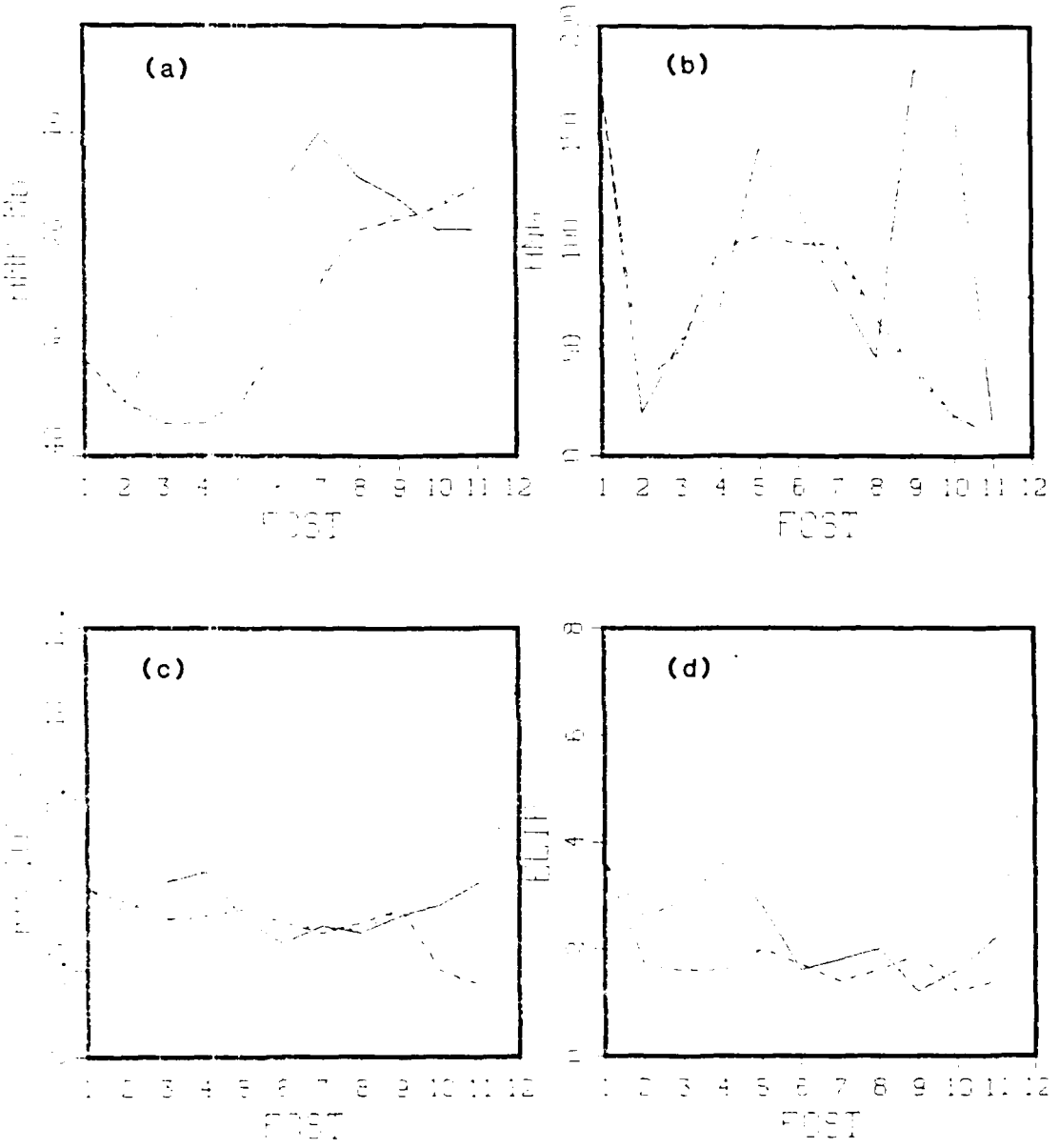

49. Similar to Fig. 27, except for storm AA1.

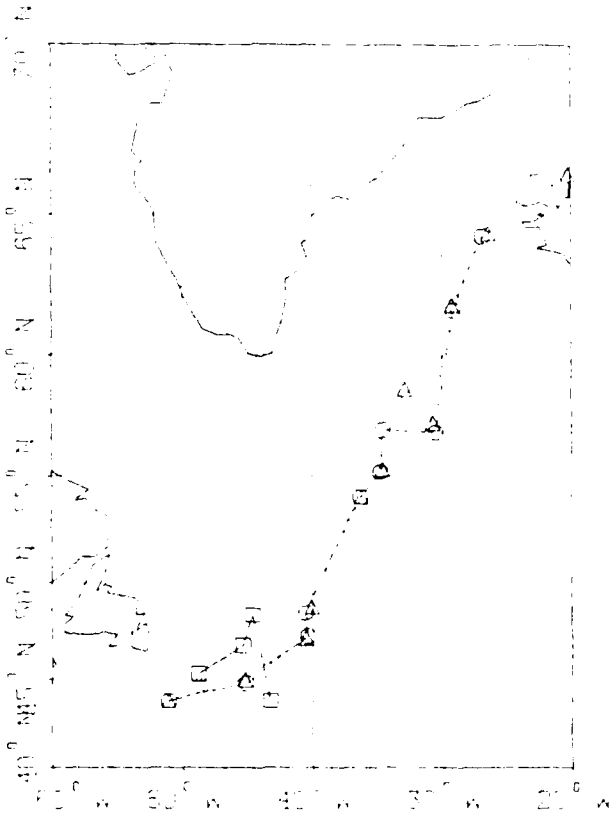

50. Similar to Fig. 26, except for storm AA2 which formed at tau= 12 hours.

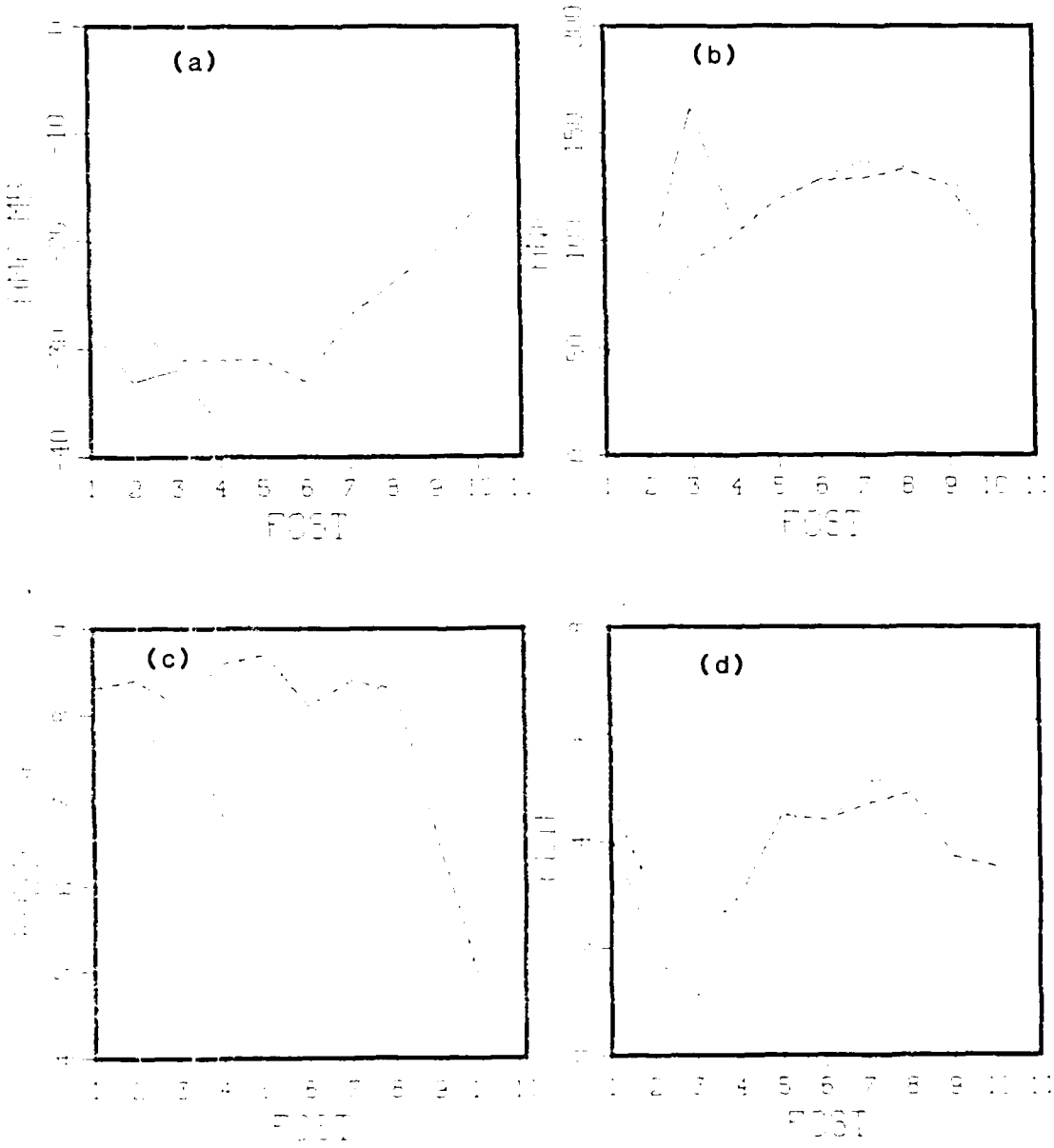

51. Similar to Fig. 27, except for storm AA2.

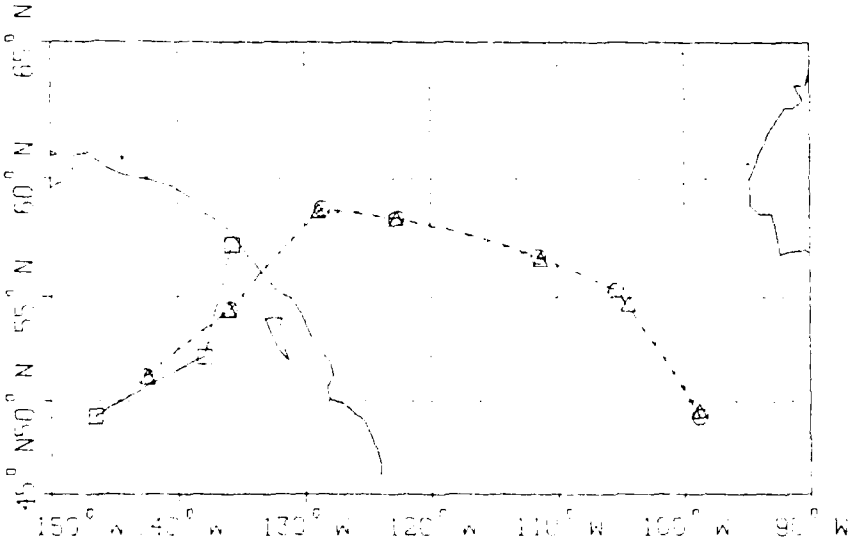

52. Similar to Fig. 26, except for storm AP1 which formed at tau= 24 hours.

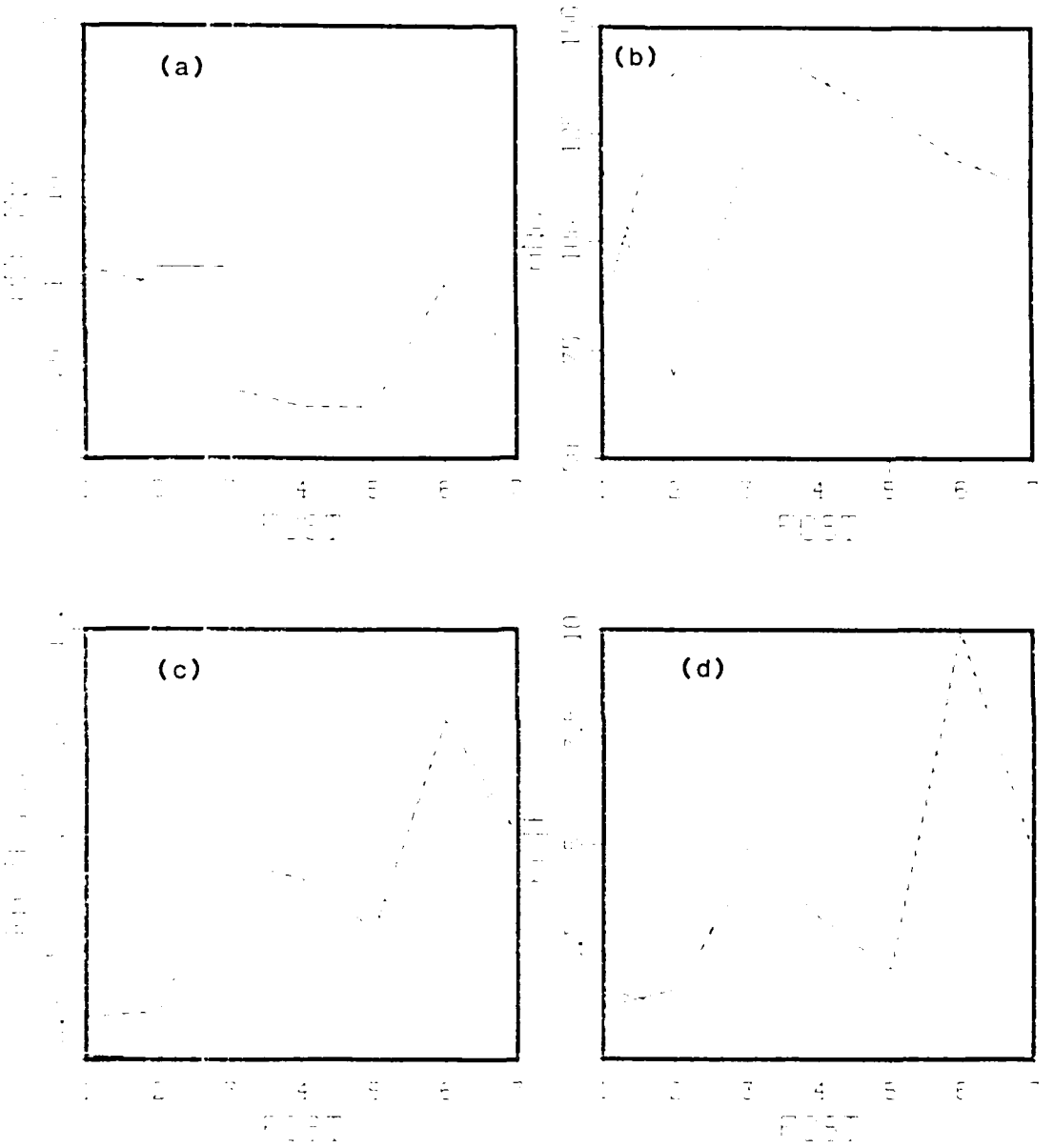

53. Similar to Fig. 27, except for storm AP1.

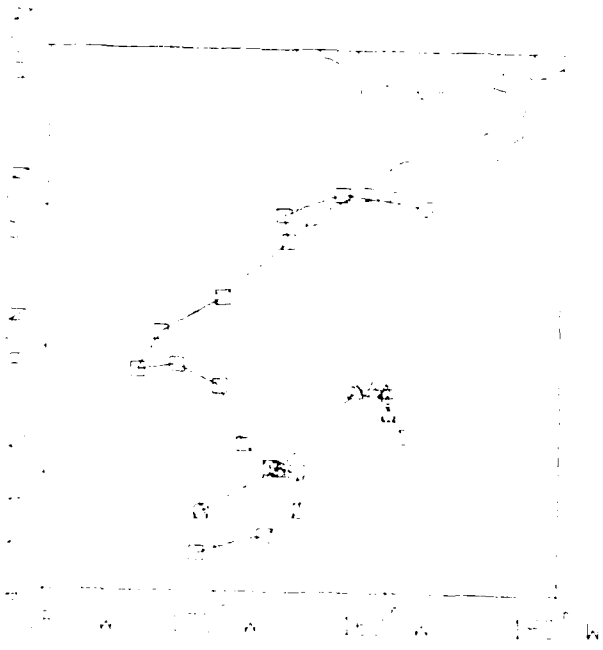

54. Similar to Fig. 26, except for storm AP2 which formed at tau= 48 hours.

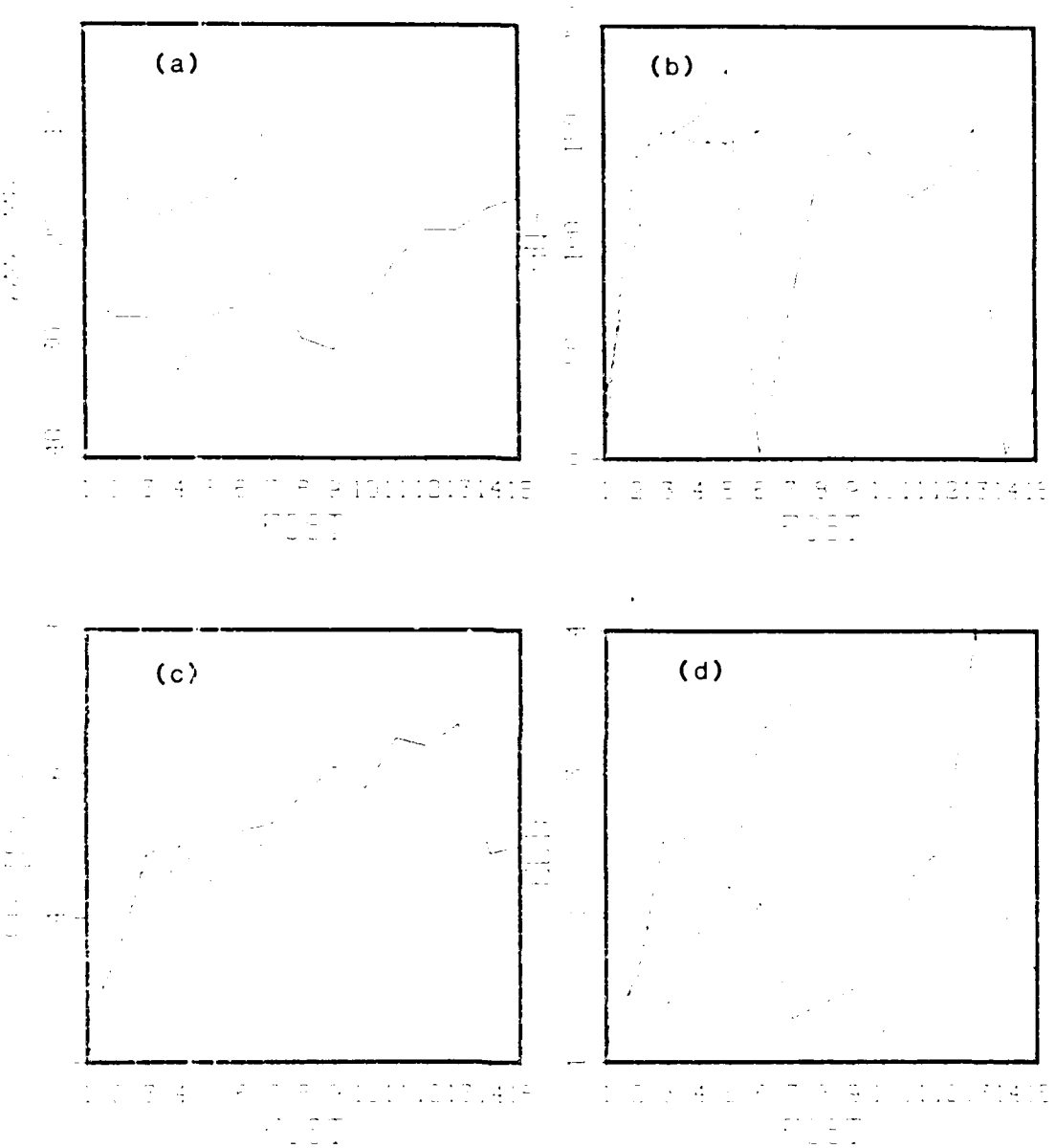

59. Similar to Fig. 27, except for storm AP2.

REFERENCES

Arpe, K.V., 1981: Impact of sea-surface temperature anomaly on medium-range weather forecasts. Unpublished report, European Center for Medium-Range Weather Forecasts, 8 pages plus 14 figures.

Bosse, T.E., 1984: Estimation of diabatic heating for an explosively-generating maritime cyclone. M.S. Thesis, Dept. of Meteorology, Naval Postgraduate School, Monterey, CA.

Brody, L.R., et al., 1984: Automated verification of numerical weather prediction forecasts - A decision aid for the operational forecaster. Preprint volume, 10th Conference on Weather Analysis and Forecasting, Tampa, FL., published by the American Meteorological Society, Boston, MA., 424-427.

Camp, N.T., and R.L. Elsberry, 1978: Oceanic thermal response to strong atmospheric forcing II. The role of one-dimensional processes. J. Phys. Oceanogr., 8, 215-224.

Clancy, R.M., and K.D. Pollack, 1983: A real time synoptic ocean thermal analysis/forecast system. Prog. Oceanogr., 12, 383-424.

Deardorff, J.W., 1972: Parameterization of the planetary boundary layer for use in general circulation models. Mon. Wea. Rev., 100, 93-106.

Elsberry, R.L., and N.T. Camp, 1978: Oceanic thermal response to strong atmospheric forcing. Part I. Characteristics of forcing events. J. Phys. Oceanogr., 8, 206-214.

Elsberry, R.L., and S.D. Raney, 1978: Sea-surface temperature response to variations in atmospheric wind forcing. J. Phys. Oceanogr., 8, 881-887.

Elsberry, R.L., et al., 1982: Ocean/Troposphere/Stratosphere Forecast Systems: A State of the Art Review. Technical Report CR 8204, Systems and Applied Sciences Corporation, 570 Casanova Ave., Monterey, CA., 79 pp.

Fanelli, P.M., 1984: Response of an atmospheric prediction model to time-dependent sea-surface temperatures. M.S. Thesis, Dept. of Meteorology, Naval Postgraduate School, Monterey, CA.

Fosmond, T.E., et al., 1983: Coupled ocean-atmosphere modeling for 3-15 day numerical prediction: A workshop report. NEPRF Tech. Rept. TR 8305, NEPRF, Monterey, CA, 81 pp.

Sanders, F., and J.R. Gyakum, 1980: Synoptic dynamic climatology of the "bomb". Mon. Wea. Rev., 108, 1589-1606.

Sandgathe, S.A., 1981: A numerical study of the role of air-sea fluxes in extratropical cyclogenesis. Ph. D. Thesis, Dept. of Meteorology, Naval Postgraduate School, Monterey, CA.

Williamson, D.L., 1981: Storm track representation and verification. Tellus, 33, 513-530.

AD-A152 020 SIMULATION OF A SYNCHRONOUSLY COUPLED ATMOSPHERE-OCEAN PREDICTION MODEL(U) NAVAL POSTGRADUATE SCHOOL MONTEREY CA P J ROVERO SEP 84 2/2

UNCLASSIFIED F/G 4/2 NL

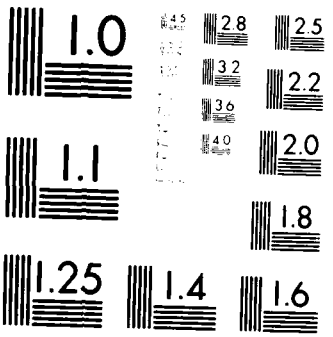

INITIAL DISTRIBUTION LIST

		No. Copies
1.	Defense Technical Information Center Cameron Station Alexandria, VA 22314	2
2.	Library, Code 0142 Naval Postgraduate School Monterey, CA 93943	2
3.	Chairman, (Code 63Rd) Department of Meteorology Naval Postgraduate School Monterey, CA 93943	1
4.	Chairman, (Code 68Mr) Department of Oceanography Naval Postgraduate School Monterey, CA 93943	1
5.	Director Naval Oceanography Division Naval Observatory 34th and Massachusetts Avenue, NW Washington, D.C. 20390	1
6.	Commander Naval Oceanography Command NSTL Station Bay St. Louis, MS 39522	1
7.	Commanding Officer Naval Oceanographic Office NSTL Station Bay St. Louis, MS 39522	1
8.	Commanding Officer Fleet Numerical Oceanography Center Monterey, CA 93943	1
9.	Commanding Officer Naval Ocean Research and Development Activity NSTL Station Bay St. Louis, MS 39522	1
10.	Commanding Officer Naval Environmental Prediction Research Facility Monterey, CA 93943	1
11.	Chairman, Oceanography Department U.S. Naval Academy Annapolis, MD 21402	1
12.	Chief of Naval Research 800 N. Quincy Street Arlington, VA 22217	1

13.	Professor R.L. Elsberry, Code63Es Department of Meteorology Naval Postgraduate School Monterey, CA 93943	5
14.	C.S. Liou, Code 63Lu Department of Meteorology Naval Postgraduate School Monterey, CA 93943	1
15.	LCDR P.H. Ranelli USS New Jersey BB-62 FPO San Francisco 96688-1110	1
16.	LT P.J. Rovero Naval Oceanography Command Detachment U.S. Naval Air Station FPO New York 09523	2
17.	Dr. T.E. Rosmond Naval Environmental Prediction Research Facility Monterey, CA 93943	1
18.	Dr. T.L. Tsui Naval Environmental Prediction Research Facility Monterey, CA 93943	1
19.	Mr. Patrick Harr Naval Environmental Prediction Research Facility Monterey, CA 93943	1

END

FILMED

5-85

DTIC